CBPF-NF-003/82

MAGNETIC FIELD INFLUENCE ON THE SPIN-PEIERLS INSTABILITY IN THE QUASI D=1 MAGNETOSTRICTIVE XY MODEL: THERMODYNAMICAL PROPERTIES

by

Raimundo Alexandre Tavares de LIMA*§ and
Constantino TSALLIS*

* Centro Brasileiro de Pesquisas Físicas/CNPq
Rua Xavier Sigaud 150, 22290 Rio de Janeiro

§ Departamento de Física, Universidade Federal de São Carlos
Via Washington Luiz Km 235, São Carlos (SP), Brazil

ABSTRACT

We study in detail within the adiabatic approximation for the structural degrees of freedom and on exact grounds for the magnetic ones, the d=1 magnetostrictive spin $\frac{1}{2}$ XY model in the presence of an external magnetic field along the Z-axis. We calculate the specific heat, magnetization, isothermal susceptibility and the structural order parameter and spectrum (including the sound velocity). The system presents, in the temperature- field space, three structurally different phases, namely the uniform (U), the dimerized (D) and the modulated (M) ones (the latter can be either commensurate or incommensurate with the other two). The critical frontiers U-D and U-M are of the second-order type while the D-M one is of the first-order type; all three join on a Lifshitz point. The U-M frontier presents a new type of multicritical point on which the frozen structural wave vector vanishes. The phase diagram is quite anomalous for high values of the elastic constant. Several other effects are predicted. The present theory is expected to be applicable to substances like TTF-BDT, MEM $(TCNQ)_2$ and eventually alkali-TCNQ.

I- INTRODUCTION

In the last decade a considerable amount of work has been dedicated to the study of the so called spin-Peierls instability (SPI) (for an excellent recent review see Bray et al[1]) which induces structural phase transitions in systems which, in what concerns magnetic interactions, are quasi-one-dimensional although three-dimensional in what concerns crystalline interactions. Typically the systems present an uniform (U) phase (referred to as the disordered one from Landau's standpoint; it corresponds to equidistant atoms along the chain) at high temperatures and a more complex phase (referred to as the ordered one) at low temperatures; this phase can be structurally dimerized (D phase) or can present complex structural modulations (M phase) according to external parameters such as the magnetic field[2-5]. The structure of the M phase might be either commensurate or incommensurate[6-9] with that of the U phase; in any case the problem is quite analogous with that of systems presenting Peierls instability[7,10-12]. The spin-Peierls type of structural phase transition has been exhibited on several substances, particularly on the TTF-BDT[4,13-17](TTF^+ - MX_4 C_4 $(CF_3)_4^-$ with (M,X) = (Cu,S), (Au,S) and (Cu,Se); TTF = tetrathiafulvalenium) and A-TCNQ (A-tetracyanoquinodimethane with A = Na, K, Rb, Cs and NH_4[18-24]; within certain restrictions we could include herein A =$MEM_{1/2}$[25-28], NMP[29], TTF[30]; MEM^{++} = N - methyl - N-ethyl - morpholinium; NMP = N - methyl - phenazinium) families through magnetic susceptibility[13,18,21,25,27,29], electrical conductivity[18-20,22,25,29], specific heat[15,27,29,30], magnetization[14,17], latent heat[18], optic properties[20,22], X-ray[14], neutron scattering[14,17] and EPR[13,18] experiments. The theoreti cal approaches to this phenomenon have been performed through use of the magnetostrictive quantum XY[2,3,5,31-37] and Heisenberg [3,7,34,38-45] models; the former, although less frequently realistic, presents the advantage of being exactly solvable in what concerns the magnetic degrees of freedom. For both models, and more particularly for the Heisenberg one, preliminary or detailed discussions have been performed concerning various quantities such as entropy[38], specific heat[3,38,45], magnetization[34,38] magnetic susceptibility[3,32,38,42,44,45], structural order parameter[3,11,32,35,36,39-41] as well as the influence, on some of them, of an external magnetic field[2,3,10,34,38,40,43,44] and of an external stress[2,51].

Let us now concentrate on the magnetostrictive spin $\frac{1}{2}$ XY model where the magnetic coupling constants are assumed to depend only on the mean distances between spins (adiabatic approximation[46]), i.e. the structural fluctuations are neglected; this assumption is expected to be acceptable if we take into account that the system is three-dimensional in what concerns the crystalline degrees of freedom. Pincus[31] showed that an XY antiferromagnetic chain is, at vanishing temperature, unstable with respect to dimerization. Beni and Pincus[32] exhibited next that this instability induces a second order phase transition between the U and D phases, under the assumption that no other phases have to be considered. Dubois and Carton[33] proved next that, at the critical temperature T_c and coming from high temperatures, appears a structural order which indeed is a dimerization. Finally in a recent paper[36] we have exhibited that below T_c down to $T = 0$, no-other contributions to the structural order appear than the pure dimerization one; the same statement seems to be true [37] in the presence of an XY coupling anisotropy[33,35].

If a magnetic field H (perpendicular to the XY plane) is applied to the system, important modifications appear in the equilibrium configuration, as the wave vector q_c characterizing the "frozen" structure might no longer be that which corresponds to a dimerization, and consequently phase transitions towards a new phase, namely the M one, might occur. The H - dependence of q_c has already been detected both theoretically[2,3,5] and experimentally[4], however the available discussions can be considered as preliminary ones. Within this respect we have recently[5] presented the complet phase diagram in the T - H space (all three U, D and M) where two special points clearly appear, one of them being a Lifshitz one, the other one, referred to as starting point, has a nature which we attempt to elucidate herein (Section IV). Furthermore in Section II we present all the details concerning this phase diagram; the influences of T, H, the harmonic and anharmonic elastic constants on the dimerization order parameter (Section III) and on the specific heat, magnetization, isothermal magnetic susceptibility, sound velocity and relevant optic frequency (Section V) are discussed as well.

II- UNIFORM CHAIN

Let us consider a cyclic linear chain (with unitary fixed crystalline parameter) of spins $\frac{1}{2}$ whose magnetic contribution to the Hamiltonian is given by

$$\mathcal{H}_m = -\sum_{j=1}^{2N} J_j(S_j^x S_{j+1}^x + S_j^y S_{j+1}^y) - \mu H \sum_{j=1}^{2N} S_j^z \qquad (1)$$

where μ is the elementary magneton, $H > 0$ by convention $\{J_j\}$ are local exchange integrals and where, for future convenience, we have considered an even number of spins. Through the Jordan-Wigner transformation[47]

$$a_j = \left(\prod_{i=0}^{j-1} 2S_i^z\right) S_j^+ \qquad (2)$$

we may introduce pseudo-fermion (spinless magnetic excitations) creation (a_j^+) and annihilation (a_j) operators, and rewrite the Hamiltonian as follows:

$$\mathcal{H}_m = -\frac{1}{2}\sum_{j=1}^{2N} J_j(a_j^+ a_{j+1} + a_{j+1}^+ a_j) + \mu H \sum_{j=1}^{2N} a_j^+ a_j - N\mu H \qquad (3)$$

where the additive term comes from the transformation

$$S_j^z = \frac{1}{2} - a_j^+ a_j \qquad (4)$$

By introducing next the Fourier transformed quantities

$$b_k = \frac{1}{\sqrt{2N}} \sum_{j=1}^{2N} e^{ijk} a_j \qquad (-\pi<k\leq\pi) \tag{5}$$

and

$$J_q = \frac{1}{2N} \sum_{j=1}^{2N} e^{ijq} J_j \qquad (-\pi<q\leq\pi) \tag{6}$$

the Hamiltonian becomes

$$\mathcal{H}_m = \mathcal{H}_o + V \tag{7}$$

where

$$\mathcal{H}_o \equiv |J_o| \left\{ \sum_k \varepsilon_k b_k^+ b_k - Nh \right\} \tag{8}$$

(this contribution is the only one in the uniform phase) and

$$V \equiv |J_o| \sum_{q\neq 0} \sum_k \Lambda_{kq} b_k^+ b_{k-q} \tag{9}$$

with

$$\varepsilon_k \equiv h - \cos k \tag{10}$$

$$h \equiv \mu H/|J_o| \tag{11}$$

$$\Lambda_{kq} \equiv -\frac{1}{2} \frac{J_q}{|J_o|} \left[e^{ik} + e^{i(q-k)} \right] \tag{12}$$

The present treatment holds for both $J_o > 0$ and $J_o < 0$, however strictly speaking the Eq. (8) is correct as it stands only for $J_o > o$; in the case $J_o < 0$ one can introduce a description in terms of holes (instead of particles)[48] and verify that the Hamiltonian remains equivalent to that of Eq. (8) excepting for the sign of the magnetic field.

Let us now calculate the magnetic contribution F_m to the free energy of the system by treating V as a pertubation to $\mathcal{H}_o$ within the temperature dependent Green functions framework [49]; we obtain

$$F_m = F_o^{(1)} + F_2^{(1)} + F_4^{(1)} + \ldots \qquad (13)$$

where $F_o^{(1)}$ is the magnetic free energy associated with $\mathcal{H}_o$, (the superscript (1) has been introduced for future convenience, and refers to the fact that the unitary crystalline cell under consideration contains only one atom), symmetry excludes odd-order terms and

$$F_j = -\frac{k_B T}{j!}\left(\frac{-1}{\hbar}\right)^j \int_0^{\hbar/k_BT} d\tau_1 \ldots \int_0^{\hbar/k_BT} d\tau_j \langle T_\tau[V_{int}(\tau_1)\ldots V_{int}(\tau_j)\rangle_{con}$$

$$(j = 2,4,\ldots) \qquad (14)$$

where T_τ is the chronological operator, the subscript of the thermal mean value $\langle\ldots\rangle_{con}$ denotes that only connected diagrams are to be considered and

$$V_{int} = e^{\mathcal{H}_o \tau/\hbar}\; V\; e^{-\mathcal{H}_o \tau/\hbar} \qquad (15)$$

In the expansion (13) we shall retain only the first two terms ($F_2^{(1)}$ corresponds to a simple two-vertex ring diagram) as we are presently interested only in the detection of the structural mode (characterized by its wave vector q) responsible for an eventual instability of the system; later on we shall come back onto this point.

We obtain (through use of tho quasi-continuum limit $\sum_k \to \frac{N}{\pi}\int_{-\pi}^{\pi} dk$)

$$f_0^{(1)} \equiv \frac{F_0^{(1)}}{N|J_0|} = -\frac{2t}{\pi}\int_0^{\pi} dk\ \ell n(2\ \mathrm{ch}\,\varepsilon_k/2t \qquad (16)$$

and

$$f_2 \equiv \frac{F_2}{N|J_0|} = \frac{1}{\pi}\sum_{q\neq 0}\int_0^{\pi} dk\ |\Lambda_{kq}|^2\ G\ (k,q) \qquad (17)$$

where

$$t \equiv k_B T/|J_0| \qquad (18)$$

and

$$G\ (k,q) = \frac{t}{2}\sum_{\omega_n}\frac{1}{(i\omega_n-\varepsilon_k)(i\omega_n-\varepsilon_{k-q})} \qquad (19)$$

where $\omega_n = t\pi(2n+1)$ with $n = 0, \pm 1, \pm 2, ...$

Through standard complex plane integration and use of Eq. (12) we finally obtain

$$f_2 = -\frac{1}{2\pi}\sum_{q\neq 0}\left|\frac{J_q}{J_0}\right|^2\int_0^{\pi} dk\ \cos^2 k\ \frac{\mathrm{th}\frac{\varepsilon_{k+(q/2)}}{2t} - \mathrm{th}\frac{\varepsilon_{k-(q/2)}}{2t}}{\varepsilon_{k+(q/2)}-\varepsilon_{k-(q/2)}} \qquad (20)$$

Let us now take into account the elastic contribution F_e to the free energy of the system. Contrarily to the magnetic contribution, this one is going to be treated only approximately (adiabatic approximation; see Ref.[46]) in the sense that we neglect structural fluctuations; this approach should be strongly crude if applied to a fully one-dimensional system, but is hopefully quite acceptable to describe substances which are three-dimensional from the crystalline point of view although fairly one-dimensionl in what concerns magnetic interactions. By neglecting anharmonic elastic contributions (they play a minor role as it will becomes clear further on) we have that

$$F_e = \sum_{j=1}^{2N} \frac{C}{2}(X_{j+1} - X_j)^2$$

$$= 2NC\sum_q (1-\cos q)|X_q|^2 \qquad (21)$$

where C is the first-neighbour harmonic elastic constant, X_j is the mean position of the j-th spin (with respect to its position in the uniform phase) and

$$X_q = \frac{1}{2N}\sum_{j=1}^{2N} e^{-ijq}X_j \qquad (22)$$

We can now go back to the magnetic contribution. If we assume that the interaction between first-neighbouring spins is characterized by an exchange integral J(u) where u denotes the incremental distance (with respect to that of the uniform chain) between two spins, and expand up to the linear term (higher- order terms play a minor role as it will become clear later on), i.e.

$$J(u) = J(0) + J'(0)u \tag{23}$$

we obtain the parameter J_j which appears in Eq. (1):

$$J_j = J(0) + J'(0)(X_{j+1}-X_j) \tag{24}$$

hence

$$J_q = J(0)\delta_{q,0} + J'(0)(e^{-iq}-1)X_q \tag{25}$$

where we have used Eqs. (6) and (22); remark that $J_0 = J(0)$. By substituting Eq. (25) into Eq. (20) and by taking into account Eqs. (16) and (21) we obtain the total free energy F of the system:

$$f \equiv \frac{F}{N|J_0|} = f_0^{(1)} + \frac{1}{2}\sum_{q\neq 0} \omega_q^2 \, \eta_q^2 \tag{26}$$

where

$$\omega_q^2 \equiv (1-\cos q)(K-L_q) \tag{27}$$

$$K \equiv \frac{C|J(0)|}{|J'(0)|^2} \tag{28}$$

$$L_q \equiv \frac{1}{4\pi\sin\frac{q}{2}} \int_0^\pi dk \, \frac{\cos^2 k}{\sin k} \left[\mathrm{th}\,\frac{h-\cos(k+q/2)}{2t} - \mathrm{th}\,\frac{h-\cos(k-q/2)}{2t}\right] \tag{29}$$

and

$$\eta_q \equiv 2\left|\frac{J'(0)X_q}{J(0)}\right| \tag{30}$$

The critical surface in the (t, h, K) - space which separates the disordered phase (uniform chain) from ordered phases (dimerized or modulated chain) is determined by a soft mode criterium, namely ω_{q_c} (t, h, K) = 0 (i.e. $K = L_{q_c}$ (t,h)) where q_c is the wave vector of the first (coming from the U phase) structural mode with respect to which the system becomes unstable, i.e. q_c maximizes L_q for fixed t and h. To be more precise $\omega_{q_c} = 0$ determines the meta-stability limit of the U phase; this limit coincides with the critical one if and only if we are facing a second order phase transition; this seems to be indeed the case all over the critical surface as strongly suggested by the analysis of the particular cases treated in Section III (if it is so, neglecting F_4 and higher order contribution in Eq. (13) is fully justified as long we do not enter into the ordered phases). We have illustrated in Fig. 1 the influence of t and h on the spectrum ω_q. In Figs. 2.a and 2.b we present t-h phase diagrams associated to different values of K; several iso-q_c lines are presented as well. We remark that: (a) at fixed value of h and increasing t we obtain the sequence (non U phase) - (U phase) if h < 1, and the sequence (U phase) - (non U phase) - (U phase) if h>1; the critical frontier is universal (the same for all values of K) at the first-order asymptotic contribution in the limit $t \to 0$, and is given by $h \sim 1 - t\,\ell n(2K\sqrt{\pi t}) \sim 1 - \frac{t}{2}\ell n t$; (b) at fixed value of t and increasing h we obtain, at intermediate temperatures, the unusual possibility of a sequence (non U phase) - (U phase) - (non U phase) - (U phase) if $K > K^* \simeq 0.2$; this possibility disappears for $K < K^*$; it is remarkable the fact that the same value $K^* \simeq 0.2$ separates [37] two different regimes in the γ - t phase diagrams where γ denotes a spin XY coupling anisotropy which can be introduced [33] in the model (in our present model $\gamma = 0$); (c) the iso-q_c lines cut the h-axis at points satisfying $h = \cos \frac{q_c}{2}$; this fact can be easily understood if, following along Peierls lines [50], we remark that $q_c = 2k_F$ where k_F is the Fermi wave vector of the problem (through Eq. (10) $\varepsilon_{k_F} = 0$ implies $h = \cos k_F$); (d) for a given value of K, the $q_c = \pi$ and $q_c = 0$ points are special ones: the former is an inflexion one and corresponds (as we shall illustrate further on) to a Lifshitz point where two second-order (U-D and U-M) and one first-order (D-M) critical lines converge; the latter is a peculiar one (obtained, as far as we know, for the first time and referred hereafter as <u>starting</u> point) whose characteristics will be discussed later on (it is systematically located slightly above, in what concerns h, another inflexion point); (e) the critical temperature at vanishing magnetic field (see Fig. 3) satisfies [2,33,36,37]

$$K = \frac{1}{\pi} \int_0^{\pi/2} dk \, \frac{\sin^2 k}{\cos k} \, \mathrm{th} \, \frac{\cos k}{2t} \tag{31}$$

$$\sim \begin{cases} \frac{1}{\pi} \ln \frac{1}{t} & \text{if } t \to 0 \quad (31') \\ \frac{1}{8t} & \text{if } t \to \infty \; ; \quad (31'') \end{cases}$$

Along the t - h critical line associated to a given value of K, q_c varies continuously: see Figs. 4.a and 4.b. It is interesting also to analyze the main properties of the function L_q as it does not depend on K: in Fig. 5 we present the locus, in the q_c - L_{q_c} space, of the maxima of L_q with respect to q (while t and h vary). The thermal dependence of $L_\pi(t,0)$ provides the vanishing field critical line in the t - K space (see the basal plane of Fig. 6).

III- DIMERIZED CHAIN: ORDER PARAMETER

III.1 - Equation of states:

Let us now consider the dimerized phase of our system, i.e. each unitary cell of the cristal contains now two spins (hence the crystalline parameter is twice its value in the uniform phase). The magnetic contribution to the Hamiltonian can be written as follows:

$$\mathcal{H}_m = -\sum_{j=1}^{N}\Big\{J(2\eta)\left(S^x_{2j-1}S^x_{2j}+S^y_{2j-1}S^y_{2j}\right) + J(-2\eta)\left(S^x_{2j}S^x_{2j+1} + S^y_{2j}S^y_{zj+1}\right)\Big\} - \mu H\sum_{j=1}^{N}\left(S^z_{2j-1}+S^z_{2j}\right) \tag{32}$$

where η is the dimerization or order parameter (the distances between neighbouring spins are now alternatively $(1 + 2\eta)$ and $(1 - 2\eta)$). By using as before the transformation (2) we obtain:

$$\mathcal{H}_m = -\frac{1}{2}\sum_{j=1}^{N}\Big\{J(2\eta)\left(a^+_{2j-1}a_{2j}+a^+_{2j}a_{2j-1}\right)$$

$$+ J(-2\eta)\left(a^+_{2j}a_{2j+1}+a^+_{2j+1}a_{2j}\right)\Big\}$$

$$+ \mu H\sum_{j=i}^{N}\left(a^+_{2j-1}a_{2j-1}+a^+_{2j}a_{2j}\right) - N\mu H$$

$$= -\frac{1}{2}\sum_{k}\Big\{J(2\eta)\left(\bar{e}^{ik}c^+_k\bar{c}_k+e^{ik}\bar{c}^+_k c_k\right)$$

$$+ J(-2\eta)\left(e^{-ik}\bar{c}_k^{+}c_k + e^{ik}c_k^{+}\bar{c}_k\right)\Big\}$$
$$+ \mu H\sum\left(c_k^{+}c_k + \bar{c}_k^{+}\bar{c}_k\right) - N\mu H \tag{33}$$

where $-\frac{\pi}{2} < k \leqslant \frac{\pi}{2}$ and

$$c_k \equiv \frac{1}{\sqrt{N}} \sum_{j=1}^{N} e^{i(2j-1)k} a_{2j-1}$$
$$\bar{c}_k \equiv \frac{1}{\sqrt{N}} \sum_{j=1}^{N} e^{i2jk} a_{2j} \tag{34}$$

In order to diagonalize the Halmitonian let us finally introduce new fermionic operators through the transformations

$$c_k = \frac{1}{\sqrt{2}} (\alpha_k + \beta_k)$$
$$\bar{c}_k = \frac{1}{\sqrt{2}} (\alpha_k - \beta_k) e^{i\theta_k} \tag{35}$$

where

$$\theta_k \equiv \operatorname{arctg}(\bar{\eta}\,\mathrm{tg}k) \tag{36}$$

whith

$$\bar{\eta} \equiv \left|\frac{J(2\eta) - J(-2\eta)}{J(2\eta) + J(-2\eta)}\right| \quad ; \tag{37}$$

whenever Eq. (23) holds we have

$$\bar{\eta} = 2\left|\frac{J'(0)\eta}{J(0)}\right| = \eta_\pi \tag{37'}$$

where we have used Eq. (30). The Hamiltonian becomes

$$\mathcal{H}_m = |J(0)|\left\{\sum_k \left(\varepsilon_k^\alpha \alpha_k^+ \alpha_k + \varepsilon_k^\beta \beta_k^+ \beta_k\right) - Nh\right\} \tag{38}$$

where

$$\begin{aligned} \varepsilon_k^\alpha &\equiv h - \sqrt{\cos^2 k + \bar{\eta}^2 \sin^2 k} \\ \varepsilon_k^\beta &\equiv h + \sqrt{\cos^2 k + \bar{\eta}^2 \sin^2 k} \end{aligned} \tag{39}$$

The free energy $F_0^{(2)}$ (the superindex (2) denotes di-merization) associated to this Hamiltonian is given by

$$f_0^{(2)} \equiv \frac{F_0^{(2)}}{|J(0)|N} = -\frac{2t}{\pi}\int_0^{\pi/2} dk\left[\ln 2\mathrm{ch}\frac{\varepsilon_k^\alpha}{2t} + \ln 2\mathrm{ch}\frac{\varepsilon_k^\beta}{2t}\right] \tag{40}$$

It is straightforward to see that $\bar{\eta} = 0$ provides expression (16). The total free energy is given by

$$f \equiv \frac{F}{|J(0)|N} = f_0^{(2)} + U(\bar{\eta};\alpha,\delta) \tag{41}$$

where $U(\eta;\alpha,\delta)$ is an elastic potential more general than $K\bar{\eta}^2$ in the sense that it may include even anharmonic contributions (characterized by the parameters $\alpha \geqslant 0$ and $0 < \delta \leqslant 1$); these contributions (which modify <u>absolutely nothing</u> in the results obtained in the previous Section) play, for small values of K, an important role as we shall see in the present Section (the role played by <u>odd</u> anharmonic contributions is a relatively secondary one and is neglected herein). In order to perform numerical applications we shall adopt

$$U(\bar{\eta};\alpha,\delta) = K\left[\bar{\eta}^2 + \frac{\alpha\bar{\eta}^4}{1-\frac{\bar{\eta}^2}{\delta^2}}\right] \qquad (42)$$

which provides $K\bar{\eta}^2$ if $\alpha = 0$, diverges if $\bar{\eta}$ grows up to δ and whose asymptotic expansion in the limit $\bar{\eta} \to 0$ is given by $K(\bar{\eta}^2+\alpha\bar{\eta}^4)$.
To be precise let us point out that the inclusion of anharmonic terms in the variable $\bar{\eta}$ (<u>instead of η</u>) <u>simultaneously</u> covers possible departures of F_e/N from $C(2\eta)^2$ and of $J(u)$ from $J(0) + J'(0)u$ (see Eq. (23)): this fact becomes clear if we remember the definition (37). According to our choice of an unitary crystalline parameter, $|\eta|$ can by no means exceed 1/2 (a physically acceptable F_e should diverge at this point); in the (highly probable) case that $J(u)$ (or $J(-u)$) vanishes before reaching up to this point, necessarily $\delta = 1$ because $|\bar{\eta}|$ can grow up to unity (see Eq. (37)); in the (speculative) case that $J(u)$ could remain finite up to $|\eta| = 1/2$ then $\delta = |J(1) - J(-1)|/|J(1) + J(-1)| < 1$.

The equation of equilibrium states $\partial f/\partial\bar{\eta} = 0$ eventually admits, besides the trivial solution $\bar{\eta} = 0$ (U phase), the following one:

$$\frac{\partial f_0^{(2)}}{\partial(\bar{\eta}^2)} + \frac{\partial U}{\partial(\bar{\eta}^2)} = 0 \qquad (43)$$

therefore (through use of Eqs. (40) and (42))

$$K = \frac{A(\bar{\eta}^2;\alpha,\delta)}{2\pi} \int_0^{\pi/2} \frac{dk \sin^2 k}{\sqrt{\cos^2 k + \bar{\eta}^2 \sin^2 k}} \left(\text{th} \frac{\varepsilon_k^\beta}{2t} - \text{th} \frac{\varepsilon_k^\alpha}{2t} \right) \qquad (43')$$

where

$$A(\bar{\eta}^2;\alpha,\delta) \equiv \left\{ 1 + \frac{\alpha\bar{\eta}^2\left(2 - \frac{\bar{\eta}^2}{\delta^2}\right)}{\left(1 - \frac{\bar{\eta}^2}{\delta^2}\right)^2} \right\}^{-1} \qquad (44)$$

This equation (discussed in subsections III. 2 and III. 3) provides, for given values of K, α and δ, the order parameter $\bar{\eta}(t,h)$ in the dimerized phase (by definition $\bar{\eta} > 0$): see Figs. 7.a and 7.b.

III.2 - Vanishing temperature

The discussion of the case $t = 0$ is rather complex and it is useful to separately describe 6 cases respectively associated with 6 different possibilities for the pseudo-fermion spectrum (see Fig. 8). Let us first point out that in the cases (c) and (f) no solution $\bar{\eta} \neq 0$ exists. The solution in the other four cases ((a), (b), (d), (e); see Fig 9) satisfies

$$K = \frac{A}{\pi} \int_{k_m}^{k_M} \frac{dk \sin^2 k}{\sqrt{\cos^2 k + \bar{\eta}^2 \sin^2 k}} \qquad \left(0 \leq k_m \leq k_M \leq \frac{\pi}{2}\right) \qquad (45)$$

Let us first of all discuss the case $\alpha = 0$ $(\forall\delta)$: Eq. (45) becomes

$$K = \begin{cases} \left. \dfrac{F(k,\sqrt{1-\bar{\eta}^2}) - E(k,\sqrt{1-\bar{\eta}^2})}{\pi(1-\bar{\eta}^2)} \right|_{k_m}^{k_M} & \text{if } \bar{\eta} \leqslant 1 \quad (46) \\ \left. \dfrac{\bar{\eta}^2 E\left(k,\dfrac{\sqrt{\bar{\eta}^2-1}}{\bar{\eta}}\right) - F\left(k,\dfrac{\sqrt{\bar{\eta}^2-1}}{\bar{\eta}}\right)}{\pi\bar{\eta}\ (\bar{\eta}-1)} \right|_{\frac{\pi}{2}-k_M}^{\frac{\pi}{2}-k_m} & \text{if } \bar{\eta} \geqslant 1 \quad (46') \end{cases}$$

where $F(x,y)$ and $E(x,y)$ respectively denote the elliptic integrals of the first and second kind, and where

$k_m = 0$ and $k_M = \pi/2$ in the cases (a) and (d),

$k_m = 0$ and $k_M = k_c$ in the case (b),

$k_m = k_c$ and $k_M = \pi/2$ in the case (e),

with

$$k_c \equiv \arcsin\sqrt{\frac{1-h^2}{1-\bar{\eta}^2}} \tag{47}$$

We remark that if $h \leqslant 1$ and $h \leqslant \bar{\eta}$ (cases (a) and (d)) Eqs. (46) and (46') imply $\bar{\eta}(0,h) = \bar{\eta}(0,0)$ where $\bar{\eta}(0,0)$ satisfies

$$K = \begin{cases} \dfrac{K\left(\sqrt{1-(\bar{\eta}(0,0))^2}\right) - E\left(\sqrt{1-(\bar{\eta}(0,0))^2}\right)}{\pi\left[1 - \left(\bar{\eta}(0,0)\right)^2\right]} & \text{if } K \geqslant \tilde{K} = \dfrac{1}{4} \quad (48) \\ \dfrac{\left[\bar{\eta}(0,0)\right]^2 E\left(\dfrac{\sqrt{(\bar{\eta}(0,0))^2-1}}{\bar{\eta}(0,0)}\right) - K\left(\dfrac{\sqrt{(\bar{\eta}(0,0))^2-1}}{\bar{\eta}(0,0)}\right)}{\pi\bar{\eta}(0,0)\ \left[(\bar{\eta}(0,0))^2-1\right]} & \text{if } K \leqslant \tilde{K} = \dfrac{1}{4} \quad (48') \end{cases}$$

where K(x) and E(x) respectively denote the complete elliptic integrals of the first and second kind; $K = \tilde{K} \equiv 1/4$ implies $\bar{\eta}(0,0) = 1$; Eq. (48) leads, in the limit $K \to \infty$, to $\bar{\eta}(0,0) \sim \frac{4}{e}\, e^{-\pi K}$; Eq. (48') leads, in the limit $K \to 0$, to $\bar{\eta}(0,0) \sim 1/\pi K$; $\bar{\eta}(0,h)$ presents two branches (see Fig. 9) which join at $h = h_M$ and we verify that $h_M \leq \bar{\eta}(0,0)$ (the equality holds if and only if $K \geq \tilde{K}$).

In the case (b), the lower branch of $\bar{\eta}(0,h)$ cuts the h-axis at $h = h_m$ (see Fig. 9) which satisfies

$$K = \frac{1}{2\pi} \ln \frac{1+\sqrt{1-h_m^2}}{1-\sqrt{1-h_m^2}} - \frac{\sqrt{1-h_m^2}}{\pi} \tag{49}$$

hence

$$h_m \sim \begin{cases} 1 - \frac{(3\pi)^{2/3}}{2} K^{2/3} & \text{if } K \to 0 \\ \frac{2}{e}\, e^{-\pi K} & \text{if } K \to \infty \end{cases} \tag{49'}$$

Let us summarize by saying that the harmonic approximation is physically acceptable for $K > \tilde{K} = 1/4$ and leads to interesting features like the evidence of first order phase transitions at vanishing temperature and $h = h^*$ $(h_m < h^* < h_M)$. On the other hand severe defects are present if $K < \tilde{K}$: we shall exhibit now that all the anomalies disappear when anharmonicity is allowed to come in $(\alpha > 0)$.

The $t = 0$ discussion of the order parameter goes, for the anharmonic case, similarly to that of the harmonic one. The results are illustrated in Figs. 10.a, 10.b, 10.c. We remark that: a) increasing α and $(1-\delta)$ lead to decreasing $\bar{\eta}(0,h)$ (in particular $\alpha \to \infty$ and/or $\delta \to 0$ imply $\bar{\eta}(0,h) \to 0$); b) $K = 0$ leads to $\bar{\eta}(0,h) = \delta \lesssim 1$ for any value of α; c) anharmonicity leads to no (to big) qualitative modifications for $K > \tilde{K} = 1/4$ $(K<\tilde{K})$; see for example the case $K = 0.4$ $(K=0.116)$ in Fig. 10.a (Figs. 9 and 10.a); d) h_m independs from α and δ (as expected if we take into accout that it concerns the limit $\bar{\eta} \to 0$) and is still given by Eq. (49); e) $h_M = \bar{\eta}(0,0)$ strongly depends on α and δ (in particular for $\delta = 1$ joins h_m in the limit $K \to 0$ for <u>any</u> positive value of α); f) within the (speculative) hypothesis $\delta < 1$, unusual sequences of two first order transitions may occur (see the case ($K = 0.116$; $\alpha = 0.5$; $\delta = 0.65$) in Fig. 10.a).

To close this subsection let us emphasize that anharmonicity is able to provide $\bar{\eta} \leq 1$ for <u>all</u> values of K as physically desirable.

III.3 - <u>Finite temperatures</u>

We shall now go back to the complete equation of states (Eq.(43')) and discuss the dimerization order parameter at finite temperatures; in order to simplify the numerical analysis we restrict to $K > \tilde{K} = 1/4$, a fact which authorizes us to neglect anharmonic contributions i.e. we adopt $\alpha = 0$ hence $A = 1$ (see Eq. (44)); the results for $K > \tilde{K}$ are qualitatively the same as long as $\alpha > 0$ (and $\delta = 1$ in order to concentrate onto the physically relevant models). The results obtained for $h = 0$ are illustrated in Fig. 6; those obtained for general values of h are illustrated in Fig. 7. We remark that for a given value of K and sufficiently high values of h, the transition ($U \leftrightarrow D$) becomes of the first order: the special point (characterized by (t_L, h_L)) which separates the second from the first order regimes appears, within the present context where no other structural order than dimerization is under consideration, like a tricritical one (in fact it will become clear later on that it is a Lifshitz point and therefore its nature is much more closer to that of a bicritical one in the sense that two second and one first order critical lines converge on it). From this point start two metastability lines, namely that of the U phase into the D phase (noted UD-line and cutting the h-axis at $h = h_m$) and that of the D phase into the U phase (noted DU-line and cutting the h-axis at $h = h_M$): see Fig. 7.c. The DU-line is of course the projection of the surface $\bar{\eta}(t,h)$ on the plane (t,h) and, if prolonged with the second order critical line, exhibits an inflexion point (which is precisely the Lifshitz one).

The first-order critical line runs between the UD - and DU-lines (see Fig. 7.c), cuts the h-axis at $h = h^*$, and is determined by the condition

$$f(t,h;\bar{\eta}(t,h)) = f(t,h;0) \tag{50}$$

therefore

$$f(0,h^*;\bar{\eta}^*) = f(0,h^*;0) \tag{50'}$$

where $\bar{\eta}^* \equiv \bar{\eta}(0,h^*) = \bar{\eta}(0,0)$. This equality leads, through use of Eq. (41) (with $\alpha = 0$), to

$$\sqrt{1-(h^*)^2}+h^* \arcsin h^* + \frac{\pi K}{2} (\bar{\eta}^*)^2 = E(\sqrt{1-(\eta^*)^2}) \tag{51}$$

which together with Eq. (48) determines η^* and h^*; we can verify a remarkable property namely

$$h^* = \sqrt{h_M h_m} \tag{52}$$

where we have used the property $h_M = \bar{\eta}(0, 0)$ and Eq. (49); in the limit $K \to \infty$ we obtain $h^* \sim \frac{2\sqrt{2}}{e} e^{-\pi K}$.

IV - MODULATED CHAIN AND STARTING POINT

Up to now we have seen that, for a given K (assumed from now on high enough to neglect anharmonicity), a critical frontier in the t-h space separates the U phase from the polymerized ones, namely the D phase (which occupies the low h zone of the ordered region, and has been the specific subject of Section III) and the M phase (which occupies the high h zone of the same region). In the present Section we intend to provide an analysis of the M phase, and more specifically concerning the two following points:

a) what is the structural order in the M phase?; b) what is the order of the transition across the U-M line? (across the U-D line the transition is a second order one; see Section III). This discussion will also enlighten the peculiar nature of the "starting point".

The full performance of this analysis demands the knowledge of the free energy as a function of an arbitrary structural order characterized by an order parameter η_q where the wave vector q might be commensurate or not with the first Brillouin zone associated with the uniform chain. In what concerns the M phase we shall restrict ourselves to two particular cases (both commensurate), namely the <u>tri</u>- and <u>tetra</u>-merized chains (respectively associated with "frozen" modes with wavevectors $q = 2\pi/3$ and $q = \pi/2$; remark that an "acoustic" mode with $q = 2\pi/3$ corresponds to an "optic" mode with $q = \pi/3$); by following along the lines of Section III we obtain the s-merized total free energy given by[2]

$$f^{(s)} = f_m^{(s)} + f_e^{(s)} \tag{53}$$

where $f_m^{(s)}$ and $f_e^{(s)}$ are respectively the magnetic free energy and the harmonic elastic potencial given by

$$f_m^{(s)} \equiv \frac{F_m^{(s)}}{|J(0)|N} = -\frac{2t}{\pi}\sum_{r=1}^{s}\int_0^{\pi/s} dk\,\ell n(1+e^{-\varepsilon_k^{(r)}/t}) \tag{54}$$

(if s=2, r=1 and r=2 respectively correspond to the previous families α and β)

and
$$f_e^{(s)} \equiv \frac{F_e^{(s)}}{|J(0)|N} = \frac{C}{|J(0)|s}\sum_{r=1}^{s}(\eta_{r+1}-\eta_r)^2 \tag{55}$$

The tri-merized (s=3) and tetra-merized (s=4) cases that we have considered have the energy spectra given by

$$\varepsilon_k^{(1)} = h - \left[\frac{\sum_{r=1}^{3}(j_r^{(3)})^2}{3}\right]^{1/2} \cos\frac{\phi_k}{3}$$

$$\varepsilon_k^{(2,3)} = h + \frac{1}{2}\left[\frac{\sum_{r=1}^{3}(j_r^{(3)})^2}{3}\right]^{1/2}\left(\cos\frac{\phi_k}{3} \pm \sqrt{3}\sin\frac{\phi_k}{3}\right) \qquad (s=3)$$

$$\phi_k \equiv \mathrm{arctg}\,\frac{\left[\left(\frac{\sum_{r=1}^{3}(j_r^{(3)})^2}{3}\right) - \left(\prod_{r=1}^{3} j_\alpha^{(3)}\right)^2\cos^2 3k\right]^{1/2}}{\left(\prod_{r=1}^{3} j_r^{(3)}\right)\cos 3k} \in [0,\pi] \tag{56}$$

and

$$\varepsilon_k^{(1,2,3,4)} = h \pm \frac{1}{2}\left\{\frac{1}{2}\sum_{r=1}^{4}(j_r^{(4)})^2 \pm \left[\frac{1}{4}\left(\sum_{r=1}^{4}(j_r^{(4)})^2\right)^2 + 2\left(\prod_{r=1}^{4} j_r^{(4)}\cos 4k\right.\right.\right.$$

$$\left.\left.\left. -(j_1^{(4)}j_3^{(4)})^2 - (j_2^{(4)}j_4^{(4)})^2\right]^{1/2}\right\}^{1/2} \qquad (s = 4)$$

(56')

where $j_\alpha^{(3,4)}$ are the reduced exchange integrals. The analysis of this two cases were performed by taking in the Eqs. (56,56') the expansion

$$j_r^{(3,4)} = 1 + \frac{J'(0)}{J(0)}(\eta_{r+1} - \eta_r) \qquad (57)$$

and assuming in the Eqs. (55,57) a sinusoidal structural order parameter - this is reasonable for not too low temperatures - given by

$$\eta_r = \eta\cos(\frac{2\pi}{s} r + \psi) \text{ with } r = 1,2,...,s \qquad (57')$$

We have used the phases $\psi = \frac{5\pi}{6}$ for $s = 3$ and $\psi = \pi$ for $s = 4$, obtained through minimization of the total free energy.

From the equilibrium condition $\frac{\partial f^{(s)}}{\partial(\eta^2)} = 0$ and Eqs. (53-57') we obtain the respective equations of states for the tri- and tetra-merized configurations:

$$K = -\frac{16}{3\pi}\sum_{\alpha=1}^{3}\int_0^{\pi/3} dk \frac{e^{-\frac{\varepsilon_k^{(r)}}{t}}}{1+e^{-\varepsilon_k^{(r)}/t}} \frac{\partial\varepsilon_k^{(r)}}{\partial(\eta_3^2)} \qquad (s = 3) \qquad (58)$$

and

$$K = - \frac{8}{\pi} \sum_{\alpha=1}^{4} \int_0^{\pi/4} dk \frac{e^{-\frac{\varepsilon_k^{(r)}}{t}}}{1+e^{-\varepsilon_k^{(r)}/t}} \cdot \frac{\partial \varepsilon_k^{(r)}}{\partial(\bar{\eta}_4^2)} \qquad (s = 4) \tag{59}$$

The results are presented in Figs. 11.a and 11.b. The transitions are of the second order on the U-M line (and only there).

Let us now conjecture what happens in the M phase. We have seen[36] in the case $h = 0$ that through the U-D critical point down to vanishing temperature there is no other structural order than pure dimerization. The same is true for $h > 0$ in the whole D phase, as no other instability than that associated with $q = 0$ (reduced Brillouin zone) is exhibited by the spectra $\omega_q(t,h,\bar{\eta}(t,h))$ and $\omega'_q(t,h,\bar{\eta}(t,h))$. At this point let us interrupt our analysis in order to indicate how the calculation of these spectra is performed. The quantities ω_q and ω'_q were obtained through a quite long but straightforward calculation of the free energy associated with Hamiltonian (1), conveniently written in the form (7), where $\mathcal{H}_0$ corresponds now to a pure dimerization (associated with the "optic" $q = 0$ mode in the reduced Brillouin zone) and where V corresponds to the rest of the modes. We treat V as a perturbation to $\mathcal{H}_0$ within the temperature dependent Green function framework, and obtain

$$\begin{aligned} \omega_q^2 &= m_q + |n_q| \\ & \qquad\qquad\qquad (-\tfrac{\pi}{2} \leq q < \tfrac{\pi}{2}) \\ \omega_q'^2 &= m_q - |n_q| \end{aligned} \tag{60}$$

where

$$m_q \equiv K + \frac{1}{2\pi}\int_0^{\pi/2} dk \Big\{ G(k,q)\Big[\cos^2(k-\theta_{k,q}) + \cos^2(k+\theta_{k,q}) -$$

$$-2\cos q \cos(k-\theta_{k,q})\cos(k+\theta_{k,q})\Big] + G'(k,q)[\sin^2(k-\theta_{k,q})+\sin^2(k+\theta_{k,q})$$

$$+ 2\cos q \quad \sin(k-\theta_{k,q}) \sin(k+\theta_{k,q})\Big]\Big\} \quad , \tag{61}$$

$$n_q \equiv K\cos q + \frac{1}{2\pi}\int_0^{\pi/2} dk \Big\{ G(k,q)\Big[e^{-iq}\cos^2(k-\theta_{k,q})$$

$$+ e^{iq}\cos^2(k+\theta_{k,q}) - 2\cos(k-\theta_{k,q})\cos(k+\theta_{k,q})\Big]$$

$$+ G'(k,q)\Big[e^{-iq}\sin^2(k-\theta_{k,q}) + e^{iq}\sin^2(k+\theta_{k,q})$$

$$+ 2\sin(k-\theta_{k,q})\sin(k+\theta_{k,q})\Big]\Big\} \tag{61'}$$

$$G(k,q) \equiv -\frac{1}{4}\Big\{ \frac{1}{\varepsilon^{\alpha}_{k+(q/2)} - \varepsilon^{\alpha}_{k-(q/2)}} \Big[\mathrm{th}\, \frac{\varepsilon^{\alpha}_{k+(q/2)}}{2t}$$

$$-\mathrm{th}\, \frac{\varepsilon^{\alpha}_{k-(q/2)}}{2t}\Big] + \frac{1}{\varepsilon^{\beta}_{k+(q/2)} - \varepsilon^{\beta}_{k-(q/2)}}$$

$$\times \Big[\mathrm{th}\, \frac{\varepsilon^{\beta}_{k+(q/2)}}{2t} - \mathrm{th}\, \frac{\varepsilon^{\beta}_{k-(q/2)}}{2t}\Big]\Big\} \tag{62}$$

and

$$G'(k,q) \equiv -\frac{1}{4}\left\{\frac{1}{\varepsilon^{\alpha}_{k+(q/2)}-\varepsilon^{\beta}_{k-(q/2)}}\left[\mathrm{th}\,\varepsilon^{\alpha}_{k+(q/2)}\right.\right.$$

$$\left.-\mathrm{th}\,\frac{\varepsilon^{\beta}_{k-(q/2)}}{2t}\right]+\frac{1}{\varepsilon^{\beta}_{k+(q/2)}-\varepsilon^{\alpha}_{k-(q/2)}}$$

$$\left.\left[\mathrm{th}\,\frac{\varepsilon^{\beta}_{k+(q/2)}}{2t}-\frac{\varepsilon^{\alpha}_{k-(q/2)}}{2t}\right]\right\} \qquad (62')$$

where ε^{α}_{k} and ε^{β}_{k} are given by Eq. (39).

Let us now take up again the conjectural discussion concerning the M phase. If we neglect solitons effects as well as eventual three-dimensional magnetic ordering ones, it is plausible that in the M phase things happen similarly to the D phase in the sense that at a given point (t,h) an unique wave vector q_M is "frozen"; iso-q_M lines are expected to exist and they should cut the U-M line at the point associated to $q_c = q_M$ (see Fig. 11.c). Within an assumption of continuity the iso-q_M lines should run along the superior (with respect to h) branch of the phase diagram associated to the fictitious uniform-polymerized transitions (see Fig. 11.b), and possibly coincide with their "first-order critical line" (see Fig. 11.c). The whole image enlightens the nature of the "starting point" and is consistent with the h-dependence (at fixed t) of the spectrum $\omega_q(t,h,\bar{\eta}(t,h))$ and $\omega'_q(t,h,\bar{\eta}(t,h))$ as illustrated in Fig. 12. Let us stress that negative values of ω_q and ω'_q denote that the order parameter which has been taken into account (the dimerization parameter $\overline{\eta}(t,h)$ in the present case) is not the appropriate one (other wave vectors are "freezing"). To say it in other words, it seems plausible that $\eta_q(t,h)$ is essentially a Dirac δ-function whose evolution at let us say $t = 0$ is as follows: for $h \leq h^*$ it is located at $q = \pi$ (extended first Brillouin zone), and while h approaches unity its location monotonically runs down to $q = 0$ (the amplitude should vanish as well in order to provide a second order phase transition).

V - DIMERIZED CHAIN: OTHER PROPERTIES

Let us now turn back to the D phase in order to discuss the T and H influence on the isochore specific heat, magnetization, isothermal magnetic susceptibility, sound velocity and the $q = 0$ "optic" frequency. We shall consider an harmonic elastic constant K high enough to neglect effects from anhamonicity.

The reduced isochore specific heat C_v is given by

$$C_v = - t\frac{\partial^2 f}{\partial t^2}\bigg|_h \tag{63}$$

where f is given by Eq. (41) (we recall that $\alpha = 0$). We obtain for $\bar{\eta} \equiv 0$ (U phase):

$$C_v = \frac{1}{4\pi t^2}\int_0^{\pi/2} dk \left\{ \frac{(h-\cos k)^2}{ch^2\frac{h-\cos k}{2t}} + \frac{(h+\cos k)^2}{ch^2\frac{h+\cos k}{2t}} \right\} \tag{64}$$

$$\sim \begin{cases} \dfrac{h^2+1/2}{4t^2} & \text{if } t \to \infty,\ \forall\ h \\[2ex] \gamma_1 \dfrac{t}{\sqrt{1-h^2}} & \text{if } t \to 0 \text{ and } h < 1 \\[2ex] \gamma_2\sqrt{t} & \text{if } t \to 0 \text{ and } h = 1 \\[2ex] \gamma_3 \dfrac{e^{-(h-1)/t}}{t^{3/2}} \left[(h-1)^2 + \gamma_4 (h-1)t + \gamma_5 t^2\right] \end{cases} \tag{64'}$$

($\gamma_1, \gamma_2, \ldots, \gamma_5$ are pure positive numbers) and for $\bar{\eta} \neq 0$ (D phase):

$$C_v = \frac{1}{4\pi t^2}\left\{\int_0^{\pi/2} dk \left[\frac{\left(\varepsilon_k^\alpha\right)^2}{ch^2\frac{\varepsilon_k^\alpha}{2t}} + \frac{\left(\varepsilon_k^\beta\right)^2}{ch^2\frac{\varepsilon_k^\beta}{2t}}\right]\right.$$

$$\left. - \frac{\left[\int_0^{\pi/2} dk\left(\frac{\varepsilon_k^\alpha}{ch^2\varepsilon_k^\alpha/2t} - \frac{\varepsilon_k^\beta}{ch^2\varepsilon_k^\beta/2t}\right)\frac{\sin^2 k}{\sqrt{\cos^2 k+\bar{\eta}^2\sin^2 k}}\right]^2}{\int_0^{\pi/2} dk\left[\left(\frac{1}{ch^2\varepsilon_k^\alpha/2t} + \frac{1}{ch^2\varepsilon_k^\beta/2t}\right) - \frac{2t(th\varepsilon_k^\alpha/2t - th\varepsilon_k^\beta/2t)}{\sqrt{\cos^2 k+\bar{\eta}^2\sin^2 k}}\right]\frac{\sin^4 k}{\cos^2 k+\bar{\eta}^2\sin^2 k}}\right\} \tag{65}$$

where ε_k^α and ε_k^β are given by Eqs. (39). Remark that C_v is univeral (the same for all K) in the U-phase. The results are presented in Figs. 13(a) and 13(b): their low temperature region compare qualitatively well with the results presented in Ref. [3]; let us stress however that the specific heat jump may occur at a temperature higher than the maximum of the corresponding universal U-phase curve (see the case K = 0.3 of Fig. 13(b)).

The reduced magnetization m is given by

$$m = -\left.\frac{\partial f}{\partial h}\right|_t \tag{66}$$

We obtain, for $\bar{\eta} \equiv 0$ (U phase),

$$m = \frac{1}{2\pi}\int_0^{\pi/2} dk\left(th\,\frac{h-\cos k}{2t} + th\,\frac{h+\cos k}{2t}\right) \tag{67}$$

$$\sim \begin{cases} \dfrac{h}{4t} & \text{if } t \to \infty, \ \forall h \\[2ex] \dfrac{1}{\pi}\left\{\arcsin h + \gamma_6 \dfrac{t}{\sqrt{1-h^2}}\left[e^{-\frac{\sqrt{1-h^2}}{t}\arcsin h} - e^{-\frac{\sqrt{1-h^2}}{t}\,\mathrm{arccosh}}\right]\right\} & \text{if } t \to 0 \text{ and } h < 1 \\[2ex] \dfrac{1}{2} - \gamma_7 \sqrt{t}\, e^{-\frac{h-1}{t}} & \text{if } t \to 0 \text{ and } h \geq 1 \end{cases} \tag{67'}$$

(γ_6 and γ_7 are pure positive numbers)

and, for $\bar{\eta} \neq 0$ (D phase),

$$m = \frac{1}{2\pi}\int_0^{\pi/2} dk \left\{ \mathrm{th}\,\frac{h - \sqrt{\cos^2 k + \bar{\eta}^2 \sin^2 k}}{2t} + \mathrm{th}\,\frac{h + \sqrt{\cos^2 k + \bar{\eta}^2 \sin^2 k}}{2t} \right\} \tag{68}$$

The results are presented in Figs. 14(a) and 14(b): they provide as particular cases situations which are compatible with those appearing in Fig. 2 of Ref. [34].

The reduced isothermal magnetic susceptibility χ is given by

$$\chi = \left.\frac{\partial m}{\partial h}\right|_t = -\left.\frac{\partial^2 f}{\partial h^2}\right|_t \tag{69}$$

We obtain, for $\bar{\eta} \equiv 0$ (U phase),

$$\chi = \frac{1}{4\pi t}\int_0^{\pi/2} dk \left\{ \frac{1}{\mathrm{ch}^2 \frac{h-\cos k}{2t}} + \frac{1}{\mathrm{ch}^2 \frac{h+\cos k}{2t}} \right\} \tag{70}$$

$$\sim \begin{cases} \dfrac{1}{4t}\left(1 - \dfrac{h^2}{4t^2}\right) & \text{if} \quad t \to \infty, \ \forall h \\ \\ \dfrac{1}{\pi\sqrt{1-h^2}} & \text{if} \quad t \to 0 \text{ and } h < 1 \\ \\ \gamma_8 \dfrac{e^{-\frac{h-1}{t}}}{\sqrt{t}} & \text{if} \quad t \to 0 \text{ and } h \geq 1 \end{cases} \tag{70'}$$

(γ_8 is a pure positive number)

and, for $\bar{\eta} \neq 0$ (D phase),

$$\chi = \frac{1}{2\pi t}\left\{\int_0^{\pi/2} dk \left(\frac{1}{ch^2 \varepsilon_k^\alpha/2t} + \frac{1}{ch^2 \varepsilon_k^\beta/2t}\right)\right.$$

$$\left. - \frac{1}{2} \frac{\left[\int_0^{\pi/2} dk \left(th^2 \frac{\varepsilon_k^\alpha}{2t} - th^2 \frac{\varepsilon_k^\beta}{2t}\right) \frac{\sin^2 k}{\sqrt{\cos^2 + \bar{\eta}^2 \sin^2 k}}\right]^2}{\int_0^{\pi/2} dk \left[\left(\frac{1}{ch^2 \varepsilon_k^\alpha/2t} + \frac{1}{ch^2 \varepsilon_k^\beta/2t}\right) - 2t\left(th \frac{\varepsilon_k^\alpha}{2t} - th \frac{\varepsilon_k^\beta}{2t}\right) \frac{\sin^4 k}{\sqrt{\cos^2 k + \bar{\eta}^2 \sin^2 k}}\right]}\right\} \tag{71}$$

The results are presented in Figs. 15a, 15b and 15 c: they provide as particular cases situations which are compatible with those appearing in Fig. 5 of Tannous and Caillé Ref.[3]; let us also remark that the curves are universal (the same for all K) in the U - phase.

Finally the reduced sound velocity v is defined through

$$v \equiv \left.\frac{\partial \omega'_q}{\partial q}\right|_{q=0} \tag{72}$$

where ω'_q given by Eq.(60). The results, as well as those obtained for ω_0 (soft mode) are presented in Figs. 16a and 16b.

VI - CONCLUSION

The spin-Peierls instability which occurs in magnetica-lly quasi-dimensional and structurally three-dimensional systems (TTF-BDT, $MEM(TCNQ)_2$, alkali-TCNQ, etc) is at the origin of a great richness of thermodynamical and dynamical properties. It seems plausible[40] that the influence of the magnetic coupling being of the Heisenberg-type or rather of the XY-type is a secondary one (the same is not true[35,37] if the model approaches the Ising one). On the other hand the eventual presence of an external magnetic field (perpendicular to the XY - plane in the case of an XY - model) substantially modifies the physical characteristics of the problem. In the present paper we have, for the magnetostrictive spin - $\frac{1}{2}$ XY model, exactly taken into account the magnetic degrees of freedom (in the uniform and dimerized phases) but only approximatively taken into account the structural degrees of freedom (more precisely we have neglected structural fluctuations, a fact which should not be two crue if we consider that the system is a three-dimensional crystal; we have furthermore neglected eventual soliton effects).

We have extended (in what concerns the domains of variation of the temperature, magnetic field and harmonic elastic constant) the available results[3,7,34] for the specific heat, magnetization and magnetic susceptibility (see Figs. 13-15). Furthermore a certain amount of interesting phenomena have been exhibited (for the first time as far as we know); let us recall those which seem to be the most relevant among them:

a) The system presents, in the T-H space, three structurally different phases, namely the uniform(U), the dimerized (D) and the modulated (M) ones. In the whole region of existence of the D-phase an <u>unique</u> wave vector q_M(namely $q_M = \pi/a$ where a is the crystalline parameter of the uniform chain) characterizes the "frozen" structure; this is probably still true in the M-phase in spite of the fact that q_M continuously varies (between 0 and π/a) therein, by taking values which can be commensurate or incommensurate with the Brillouin zone associated to the U-phase.

b) The first order critical frontier which separates the D- and M-phases is such that the critical magnetic field increases (decreases) with temperature if the harmonic elastic constant is sufficiently small (large).

c) The frontier which separates the U-phase from the other two is a second order one, and presents two special points; one of them is a Lifshitz point and corresponds to the point where the relevant wave vector q_c begins to differ from π/a (it is an inflexion point of the frontier; furthermore the first order D-M-frontier joins precisely there the second order frontier); the other one, referred to as "starting point", presents a quite peculiar nature (see Fig.11 (c)) and corresponds to the point where q_c vanishes (this fact occurs at <u>finite</u> temperature). The Lifshitz and starting points monotonously approximate to each other for decreasing harmonic elastic constant.

d) For sufficiently high elastic constants, fixed temperature and increasing magnetic field it is possible to observe (see Fig.2.a) the unusual phase sequence non uniform - uniform - non uniform - uniform; for all values of the elastic constant, intermediate values of the magnetic field and increasing temperature, the sequence which occurs is U-M-U.

e) The thermal dependence of the sound velocity presents a gap at the U-D critical points (possibly at the U-M critical points as well) which considerably grows in the presence of an external magnetic field. Less spectacular effects (softening) are predicted for the q=0 "optic" frequency (some experimental indications for this softening are already available[14]).

Experimental evidences of the above effects would be very wellcome.

As a final conclusion let us present a few numerical comparisons of the present theory with other available theoretical and experimental results:

i) The location of the Lifshitz point is characterized by $T_L/T_C(H=0)$; experimental values (obtained for TTF-Au BDT, TTF- Cu BDT and MEM $(TCNQ)_2$) range between about 0.65 and 0.8 (see Ref.[1] and particularly its Fig. 24); theories from Bray[7] and Bulaevskii et al[34] provide 0.54, and that from Cross[7] provides 0.77; the present treatment yields values which range from 0.59 to 0.68 while the reduced (harmonic) elastic constant K decreases from 0.6 to 0.06.

ii) The location of the vanishing temperature critical magnetic field H_c (separating the D- and the M-phases) is characterized by $H_c/T_c(H=0)$;

this quantity is experimentally determined (for the same three substances in (i)) to be 10.5 ± 0.6[1] ([H] = KOe and [T] = ^{0}K); Bray[7] and Bulaevskii et al[34] theories provide 11.2 and Cross[7] theory provides 10.3. In terms of the present reduced variables we have $H_c/T_c(H=0) = (k_B/\tilde{g}\mu_B)(h_c/t_c(h=0)) = 7.47\, h_c/t_c(h=0)$ where we have used the gyromagnetic ratio $\tilde{g} = 2$ (EPR results[13] for TTF-Cu BDT yield $\tilde{g}$ ranging between 2.0016 and 2.0151) and Bohr magneton μ_B; $H_c/T_c(H=0)$ varies from 9.2 to 9.6 while K increases from 0.3 to 0.6.

iii) It is both experimentally and theoretically found that, in the limit $H \to 0$,

$$\frac{T_c(H=0) - T_c(H)}{T_c(H=0)} \sim \lambda \left[\frac{\mu_B H}{k_B T_c(H=0)}\right]^2 \qquad (\lambda > 0).$$

λ is theoretically determined to be 0.44 (Refs. [7] (Bray) and [34]) or 0.36 (Ref. [7] (Cross)); our treatment provides $\lambda \simeq 0.9$. A first analysis[1] of the experimental data (relative to the same three substances in (i)) was compatible with our value, while further analysis[1] was more compatible with the other two values.

iv) The vanishing field isothermal magnetic susceptibility enables also severe comparisons, for example in the region of the "knee" at T_c, namely the quantity $d[\chi(T)/\chi(T_c)]/d[T/T_c]\Big|^{D}_{T=T_c}$; experimental results (Fig. 10 of Ref. [1]) for TTF-Cu BDT provide the value 2.7; in our treatment this quantity presents, in the neighborhood of K=0.4, a maximum value of about 2.5 (its value is about 2 for both K=0.3 and K=0.6).

v) The vanishing field derivative $d\chi/dT\Big|_{T=T_c}^{U}$ could in principle be negative, however typically is positive; in this case by further increasing the temperature ($T \geqslant T_c$), χ achieves a maximum χ_{max} at $T=T_{max}$; the experimental evidence (Fig. 10 of Ref. [1]) on TTF-CuBDT provides a ratio $T_{max}/T_c \simeq 4$; in our treatment this ratio is, for $K=0.6$, 2.5 and achieves the value 4 for $K>0.6$.

vi) In what concerns the ordinates of graphs χ vs.T (vanishing magnetic field), it is possible to extrapolate, in the limit $T \to 0$, the thermal dependence of χ in the uniform phase, thus obtaining $\chi(T=0;$ extrap); the already mentioned experiment (Fig. 10 of Ref.[1]) on TTF-CuBDT provides a ratio $\chi_{max}/\chi(T=0;\text{ extrap}) \simeq 1.4$; this ratio achieves, within the present treatment, its maximum value (about 1.3) in the neighborhood of $K=0.5$.

Similarly to the other theoretical proposals available in the literature, the present one is not strictly capable of numerically reproducing, with a single set of parameters, a large variety of experimental results; this is not surprising if we take into account its intrinsic simplicity. However we have exhibited that, with values of K (quantity related to a subtle one, namely the space variation of the exchange integral) ranging from let us say 0.4 to 0.6, an overall description is possible which numerically is acceptable and which qualitatively is no doubt quite satisfactory. This fact raises (at least in our minds!) the hope that most of the predictions provided by the present theory (particularly points (a) - (e) in this Section) can be verified in nature.

REFERENCES

1- J.W. Bray, L.V. Interrante, I.S. Jacobs and J.C. Bonner, to appear in "Extended Linear Chain Compounds", Vol. III, ed. Miller (Plenum, 1982).

2- C. Tsallis, "Contribution à l'etude théorique de transitions de phase magnétiques et structurales", Doctoral Thesis. Université Paris-Orsay (1974); C. Tsallis and L. de Sèze, Ferroelectrics 14, 661(1976).

3- C. Tannous and A. Caillé, Can. J. Phys. 57, 508(1979); Y. Lépine, C. Tannous and A. Caillé, Phys. Rev. B 20, 3753(1979).

4- I.S. Jacobs, J.W. Bray, H.R. Hart, Jr., L.V. Interrante, J.S. Kasper, D. Bloch, J. Voiron, J.C. Bonner, D.E. Moncton and G. Shirane, J. Mag. Mag. Mat. 15-18, 332(1980); D. Bloch, J. Voiron, J.C. Bonner, J. W. Bray, I.S. Jacobs and L.V. Interrante, Phys. Rev. Lett. 44, 294(1980).

5- R.A.T. Lima and C. Tsallis, to be published (Sol. State Commun. (1982)).

6- S. Aubry, "Solitons and Condensed Matter Physics" ed. A.R. Bishop and T. Schneider (Berlin; Springer, 1978).

7- J.W. Bray, Sol. State Commun. 26, 771(1978); M.C.Cross, Phys.Rev. B 20, 4606(1979).

8- A.D. Bruce and R.A. Cowley, J. Phys. C 11, 3577, 3591, 3609(1978).

9- J. Villain and M. Gordon, J. Phys. C 13, 3117(1980).

10- M.C. Leung, Phys. Rev. B 11, 4272(1975).

11- Per Bach and V.J. Emery, Phys. Rev.Lett. 36, 978(1976).

12- Y. Lépine and A. Caillé, Sol. State Commun. 28, 655(1978); A. Kotani and I. Harada, J. Phys. Soc. Japan 49, 535(1980)

13 - I.S. Jacobs, J.W. Bray, H.R. Hart, Jr., L.V. Interrante, J.S. Kasper, G.D. Watkins, D.E. Prober and J.C. Bonner, Phys. Rev. B 14, 3036(1976).

14 - D.E. Moncton, R.J. Birgeneau, L.V. Interrante and F. Wudl, Phys. Rev.Lett. 39, 507(1977); J.S. Kasper and D.E. Moncton, Phys.Rev. B, 20, 2341(1979).

15 - T. Wei, A.J. Heeger, M.B. Salamon and G.E. Delker, Sol. State Commun. 21, 595(1977).

16 - E. Ehrenfreud and L.S. Smith, Phys. Rev. B 16, 1870(1977); J.C. Bonner et al., J. Appl. Phys. 50, 1810(1979); J.N. Fields et al., J. Appl. Phys. 50, 1807(1979).

17 - J.W. Bray, L.V. Interrante, I.S. Jacobs, D.Bloch, D.E. Moncton, G. Shirane and J.C. Bonner, Phys. Rev. B20, 2067 (1979).

18 - J.G. Vegter, T. Hibma and J. Kommandeur, Chem. Phys. Let. 3, 427 (1969).

19 - N. Sakai, F. Shirotani and S. Minomura, Bull. Chem. Soc. Jap. 45, 3314 (1972).

20 - S.K. Khanna, A.A. Bright, A.F. Garito and A.J. Heeger, Phys. Rev. B10, 2139 (1974).

21 - J.G. Vegter and J. Kommandeur, Mol. Cryst. and Liq. Cryst. 30, 11 (1975).

22 - D.B. Tanner, C.S. Jacobsen, A.A. Bright and A.J. Heeger, Phys. Rev. B16, 3283 (1977).

23 - M. Konno, T. Ishii and Y. Saito, Acta Cryst. B33, 763 (1977).

24 - H. Terauchi, Phys. Rev. B17, 2446 (1978).

25 - P.I. Kuindersma, G.A. Sawatzky and J. Kommandeur, J. Phys.C8, 3005, 3016 (1975).

26 - A. Bosch and B. van Bodegon, Acta Cryst. B33, 3013 (1977).

27 - S. Huizinga, J. Kommandeur, G.A. Sawatzky, B.T. Thole, K. Kopinga, W.J.M. de Jonge and J. Roos, Phys. Rev. B19, 4723 (1979).

28 - H.A. Mook et al., Bull. Amer. Phys. Soc. 24, 507 (1979).

29 - A.J. Epstein, S. Etemad, A.F. Garito and A.J. Heeger, Phys. Rev. B5, 952 (1972).

30 - R.A. Craven, M.B. Salamon, G. De Pasquali, R.M. Herman, G. Stucky and A. Schultz, Phys. Rev. Lett. 32, 769 (1974).

31 - P. Pincus, Sol. State Commun. 9, 1971 (1971).

32 - G. Beni and P. Pincus, J. Chem. Phys. 57, 3531 (1972).

33 - J.Y. Dubois and J.P. Carton, J. Phys. 35, 371 (1974).

34 - L.N. Bulaevskii, A.I. Buzdin and D.I. Komskii, Sol. State Commun. 27, 5 (1978).

35 - Y.Lépine and A. Caillé, J. Chem. Phys. 71, 3728 (1979); Y. Lépine, Phys. Rev. B24, 5242 (1981).

36 - R.A.T. Lima and C. Tsallis, Sol. State Commun, 40, 155 (1981).

37 - C. Tsallis and D.M.H. da Silva, to be published. (1981).

38 - J.C. Bonner and M.E. Fisher, Phys. Rev. B135, A640 (1964).

39 - G. Beni, J. Chem. Phys. 58, 3200 (1973).

40 - E. Pytte, Phys. Rev. B10, 4637 (1974).

41 - Y. Lépine and A. Caillé, J. Chem. Phys. 67, 5598 (1977).

42 - Y. Lépine, A. Caillé and V. Larochelle, Phys. Rev. B18, 3585 (1978).

43 - M.C. Cross and D.S. Fisher, Phys. Rev. B19, 402 (1979).

44 - J.C. Bonner, H.W. Blöte, J.W. Bray and I.S. Jacobs, J. Appl. Phys. 50, 1810 (1979).

45 - Y. Takaoka and K. Motizuki, J. Phys. Soc. Jap. 47, 1752 (1979).

46 - C. Domb , J. Chem. Phys. 25, 783 (1956); S.R. Salinas, J. Phys. C7, 241 (1974).

47 - P. Jordan and E. Wigner, Z. Phys. 47, 631 (1928).

48 - E. Lieb, T. Schultz and D. Mattis, Ann. Phys. 16, 407 (1961).

49 - A.A. Abrikosov, L.P. Gorkov and I.E. Dzialoshinski, "Methods of Quantum Field Theory in Statistical Physics", p. 120. Dover, New York.

50 - R.E. Peierls, "Quantum Theory of Solids", (Oxford Univ. Press, London) 108(1954)

51 - J.W. Bray, Sol. State Commun. 35, 853(1980); I.S. Jacobs, J.W. Bray, L.V. Interrante, D. Bloch, J. Voiron and J.C. Bonner, "Physics in One Dimension", ed. by J. Bernasconi and T. Schneider (Springer, New York, 1981), p. 173.

CAPTION FOR FIGURES

Fig. 1 - Uniform chain relevant phonon spectra associated with sets of reduced temperature t, magnetic field h and elastic constant K. The cases I and III exhibit the trigger of incommensurate (or high-order commensurate) structural instabilities.

Fig. 2 - Critical lines (continuous) in the reduced temperature-magnetic field space; they separate, for different values of the reduced elastic constant K, the uniform (U) from the dimerized and modulated phases. Various iso-q_c lines (dashed) are indicated as well; those associated with $q_c = \pi$ and $q_c = 0$ respectively correspond to Lifshitz (full dots) and "starting" (empty dots) points. Note that the (a) and (b)scales are different.

Fig. 3 - Reduced temperature - inverse elastic constant phase diagram associated with vanishing magnetic field; (U) and (D) respectively denote the uniform and dimerized phases

Fig. 4 - Variation of the wave vector q_c (associated with the structural instability) along the critical line (q_c against the reduced temperature (a) or magnetic field (b)) associated with given values of the reduced elastic constant K ; LP and SP respectively denote Lifshitz and "starting" points; $q_c=0$ and $q_c=\pi$ respectively denote the uniform and dimerized phases. (b) the $K = \infty$ curve (dashed) satisfies $h=\cos(q_c/2)$; the $q_c=0$ variation of the $K=0.2$ line has been designed

slightly below the abcissa only for visual purposes.

Fig. 5- Locus of the maxima of L_{q_c} with respect to q_c: several isofield (continuous) and isothermal (dashed) lines are indicated. Isofield lines: (a) the vertical asymptotes (dot-dashed lines) are located at $q_c=2$ arccos h; (b) $h=0$ ($h \to \infty$) is associated with the axis $q_c=\pi$ (axis $L_{q_c}=0$). Isothermal lines: (a) all of them start, for $h=0$, on the axis $q_c=\pi$ and are partially contained therein; (b) all of them are partially contained in the axis $q_c=0$ and finish, for $h \to \infty$, at the corner $q_c=L_{q_c}=0$; (c) the $t \to 0$ ($t \to \infty$) line corresponds to $L_{q_c} \to \infty$ ($L_{q_c} \to 0$). The full (empty) dots correspond to Lifshitz ("starting") points. The numbers between parentheses are the associated values of t.

Fig. 6- Vanishing magnetic field dimerization order parameter $\bar{\eta}$ as a function of the reduced temperature t and elastic constant K; $\alpha = 0$, $\forall\ \delta$. The lower K is, more important become the anharmonic effects ($\alpha > 0$) in order to avoid an unphysical growth of $\bar{\eta}$ in the low temperature region.

Fig.7 - Dimerization order parameter $\bar{\eta}$ as function of the reduced temperature and magnetic field; $\alpha=0$, $\forall\ \delta$. (a) the projection of the surface on the $\bar{\eta}=0$ plane is indicated as well (dot-dashed). (b) isothermal lines; the dot-dashed lines indicate the $\eta\neq 0 \leftrightarrow \eta=0$ first-order phase transitions ($t=0$, 0.05, 0.1 imply $h^*=0.325$, 0.312, 0.285); (c) magnetic field-temperature phase diagram; the full and the dot-dashed lines are respectively

a second and a first order critical ones; the UD- and DU-lines are metastability limits. LP denotes the Lifshitz point.

Fig. 8 - The six typical possibilities for pseudo-fermions spectrum. At t=0 only the regions with $\varepsilon_k<0$ are populated. In (b) and (e) we have indicated the wave vector q_c.

Fig. 9 - The vanishing temperature dimerization order parameter associated, for different values of K, with the six cases (separated by dot-dashed lines) for pseudo-fermion spectrum (see Fig. 8); $\alpha=0$, $\forall\ \delta$. The lines within regions where the harmonic approximation is physically unacceptable are dashed. The small figure shows the K dependence of h_m and h_M.

Fig.10 - The effect of anarmonicity on the vanishing temperature dimerization order parameter $\bar{\eta}(0,h)$; (a) the order parameter as function of h for selected values of K, α and δ; (b) $h_M = \bar{\eta}(0,0)$ as a function of α for K=0.4 and different values of δ; (c) h_M as a function of K for $\alpha=0.5$ and different values of δ.

Fig. 11 - (a) Critical lines (continuous) in the t-h space for different values of K; the iso-q_c line (dotted) associated with the wave vector $q_c=\pi/2$ (tetra-merized modulation) is indicated as well; the dashed lines indicate the $\eta=0$ metastability limit associated with the fictitious uniform-tetramerized transition. (b) Critical line for K=0.4; the

uniform-dimerized and the (fictitious) uniform-tetramerized transitions are indicated as well (the dashed and dot-dashed lines respectively denote metastability limits and the first order critical line). (c) Phase diagram indicating the uniform (U), dimerized (D) and modulated (M) regions; the $q=\frac{2\pi}{3}$ and $q=\frac{\pi}{2}$ first-order critical lines (which possibly correspond to iso-q_M lines; see the text) are indicated (dashed) as well; the $q \simeq 0$ line is qualitative and has been included in order to characterize the nature of the starting point (SP); LP denotes the Lifshitz point.

Fig.12- Example (K=0.4) of the relevant phonon spectrum along an isothermal line (t=0.1) as a function of the magnetic field h. The cases I-VI correspond to those indicated in Fig. 7.b (cases VII-IX are not indicated therein). In case I we are in the D-phase, below the UD-line (this is the type of spectrum we observe in the entire D-phase, below the first-order DM-line); in case II we are in the M-phase, between the DM- and DU- lines; the DU- line ($\omega_0 = \omega_0' = 0$) is achieved between the II and III cases; the (unphysical) case III corresponds to the location of the DM- line (ω_0' presents its most negative value); the case IV corresponds to the UD - line ($\omega_0' = 0$); in case V we are in the M-phase, above the DU-line; in case VI we are in the U- phase; in cases VII and VIII we are oncemore in the M- phase; in case IX we are crossing the UM-line (which, above the starting point, is simultaneously an iso-q_c line as well as an iso-q_M one with $q_c=q_M=0$).

Fig. 13 - Reduced specific heat (per couple of spins and in units of k_B) as a function of temperature. (a) universal (K-independent) U-phase curves for selected values of the magnetic field; (b) vanishing magnetic field curves for selected values of the elastic constant (the dot-dashed line indicates the locus of the maxima of C_V which occur at the respective critical points).

Fig. 14 - Influence of the temperature t and magnetic field h on the reduced magnetization m (for K=0.4). Iso-field lines ((a) for $h \leq h_L < \simeq 0.258$; (b) for $h \geq h_L$): the dot-dashed line indicates the locus of the "knees" occurs at the respective critical points and the dotted-line corresponds to the first-order DM-line; although graphically not visible, the h = 1.04 line cuts twice the dot-dashed line (see Fig. 2.a). Isothermal lines (c): both $t \leq t_L \simeq 0.151$ ant $t > t_L$ are represented; the dashed part of the t = 0.1 line is qualitative as it corresponds to the M-phase where the equations of state are unknown; the t = 0.3 line lies within the uniform region; in the small figure we illustrate the magnetization saturation which occurs in the high field limit for all temperatures.

Fig. 15 - Thermal behaviour of the reduced isothermal magnetic susceptibility; (a) the universal (K-independent) U- phase curves for selected values of the magnetic field; (b) illustration, for selected values of the elastic constant K and vanishing magnetic field (appearance of a discontinuity);

the dot-dashed line represents the locus of the peaks (it suggests a divergence as the Lifshitz point is approached).

Fig.16- Thermal dependence of the $q = 0$ optical square reduced frequence (a) and the reduced sound velocity (b) for $K = 0.4$ and different values of $h \leq h_L \simeq 0.258$; in the $t \to \infty$ limit ω_0 and v respectiveiy saturate at $\sqrt{2K}$ and $\sqrt{K/2}$.

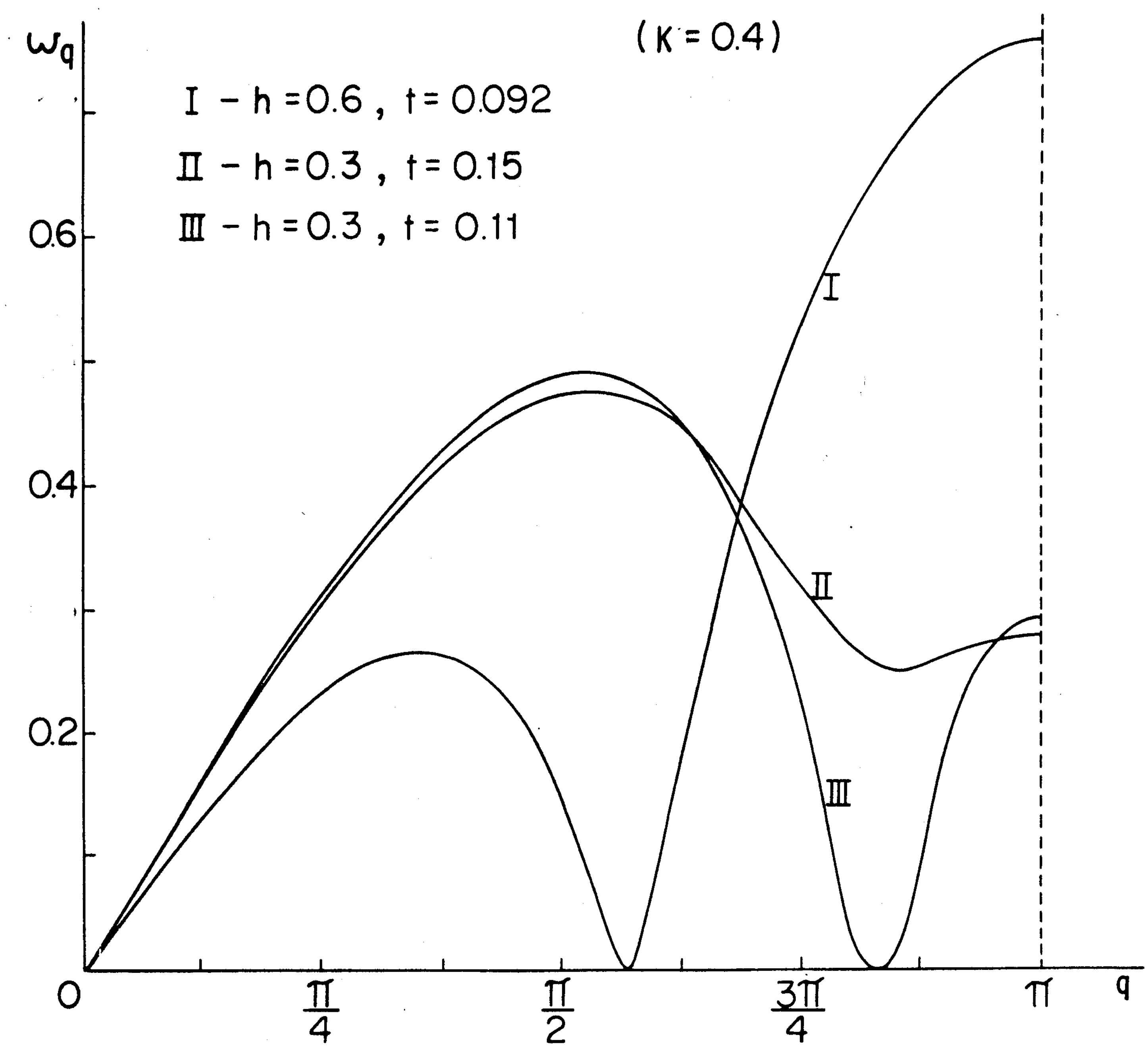

ωq
(K = 0.4)
I - h = 0.6 , t = 0.092
II - h = 0.3 , t = 0.15
III - h = 0.3 , t = 0.11
0.6
0.4
0.2
0
I
II
III
π/4
π/2
3π/4
π
q

FIG.1

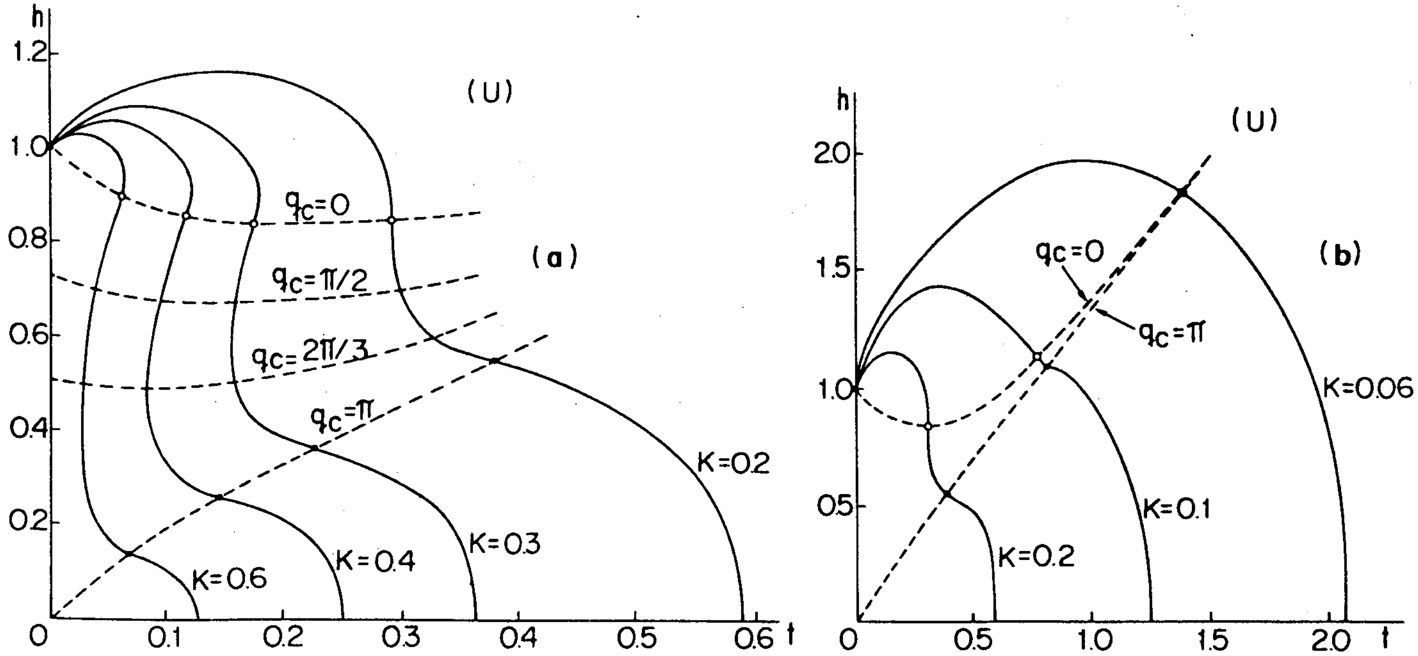
h
1.2
1.0
0.8
0.6
0.4
0.2
0
0.1
0.2
0.3
0.4
0.5
0.6
t
(U)
(a)
qc=0
qc=π/2
qc=2π/3
qc=π
K=0.6
K=0.4
K=0.3
K=0.2
h
2.0
1.5
1.0
0.5
0
0.5
1.0
1.5
2.0
t
(U)
(b)
qc=0
qc=π
K=0.06
K=0.1
K=0.2

FIG.2

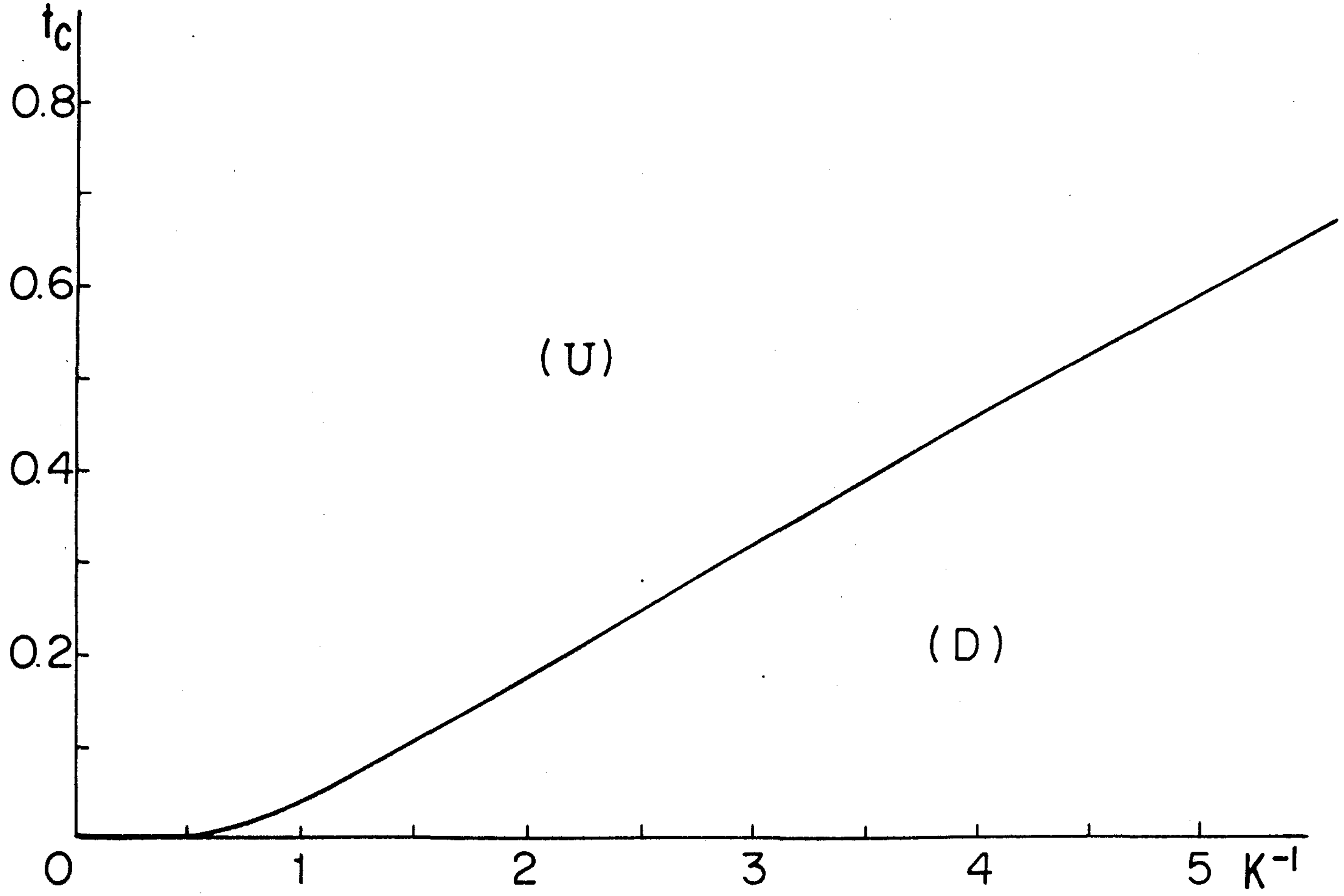

FIG. 3

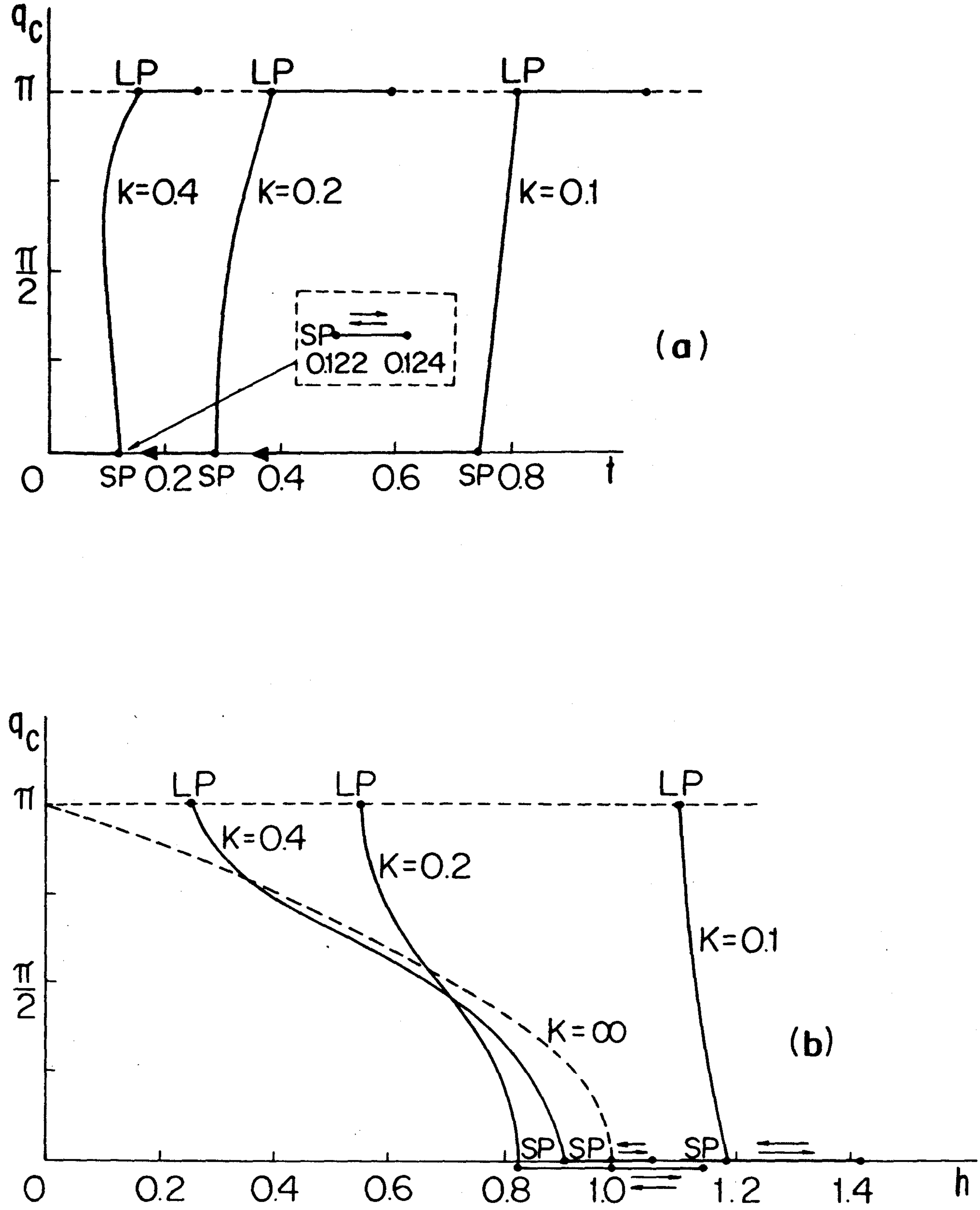

q_c
π
π/2
LP
LP
LP
K=0.4
K=0.2
K=0.1
SP
0.122
0.124
(a)
0
SP
0.2
SP
0.4
0.6
SP
0.8
t
q_c
π
π/2
LP
LP
LP
K=0.4
K=0.2
K=0.1
K=∞
(b)
SP
SP
SP
0
0.2
0.4
0.6
0.8
1.0
1.2
1.4
h

FIG. 4

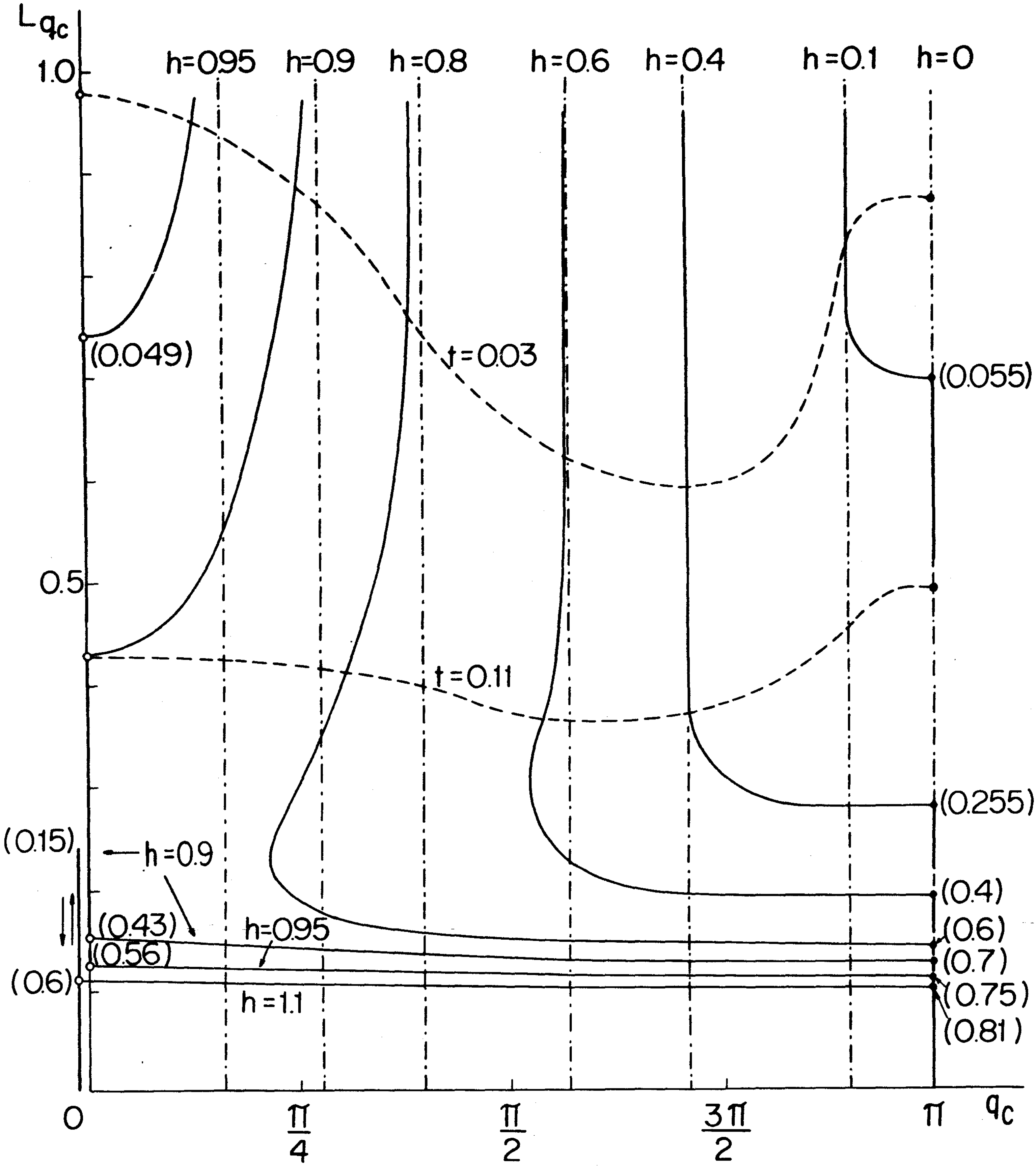
L_{q_c}
1.0
0.5
h=0.95
h=0.9
h=0.8
h=0.6
h=0.4
h=0.1
h=0
(0.049)
t=0.03
(0.055)
t=0.11
(0.255)
(0.15)
h=0.9
(0.4)
(0.43)
h=0.95
(0.6)
(0.56)
(0.7)
(0.6)
(0.75)
h=1.1
(0.81)
0
π/4
π/2
3π/2
π
q_c

FIG. 5

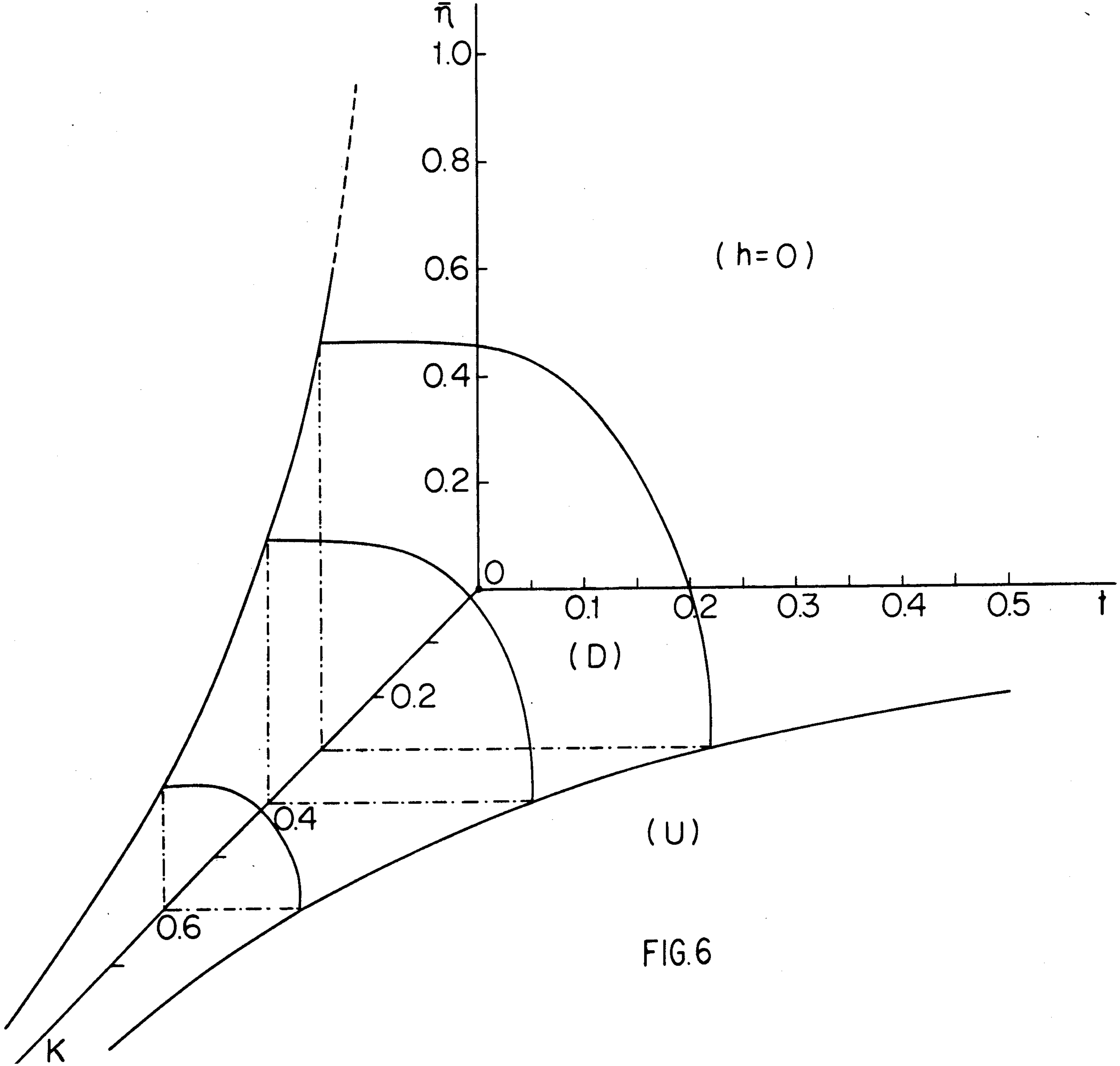

FIG.6

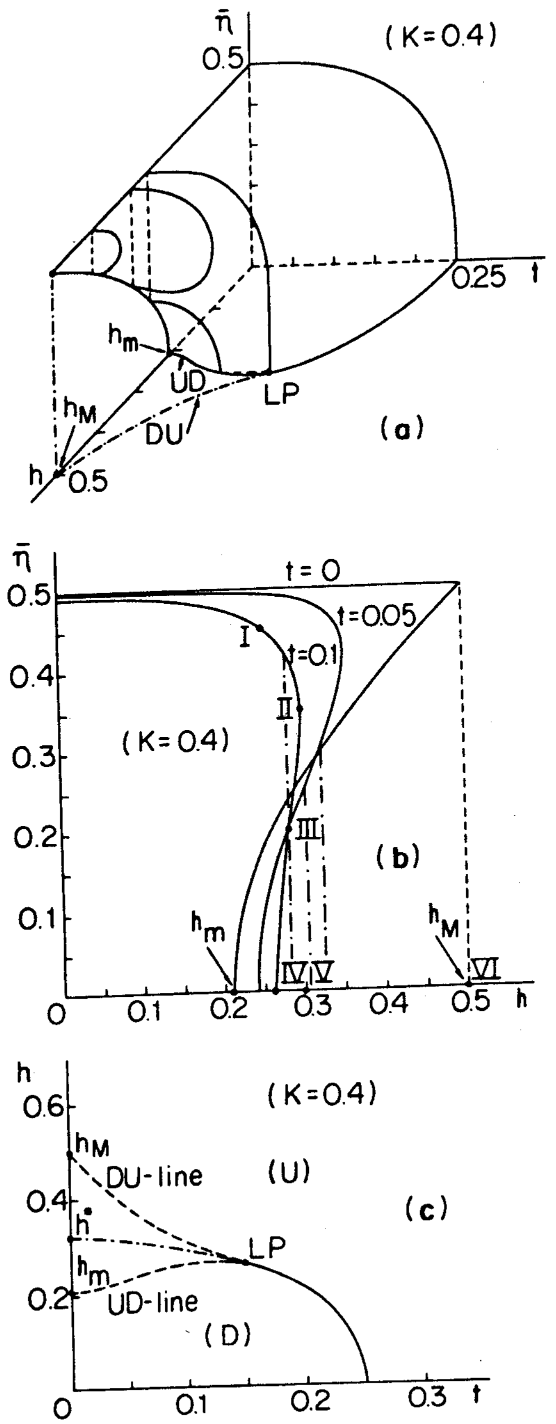

η̄
0.5
(K=0.4)
0.25
t
h_m
UD
LP
h_M
DU
(a)
h
0.5
η̄
t=0
0.5
t=0.05
I
t=0.1
0.4
II
0.3
(K=0.4)
III
0.2
(b)
0.1
h_m
h_M
IV
V
VI
0
0.1
0.2
0.3
0.4
0.5
h
h
0.6
(K=0.4)
h_M
DU-line
(U)
0.4
(c)
h*
LP
h_m
0.2
UD-line
(D)
0
0.1
0.2
0.3
t

FIG. 7

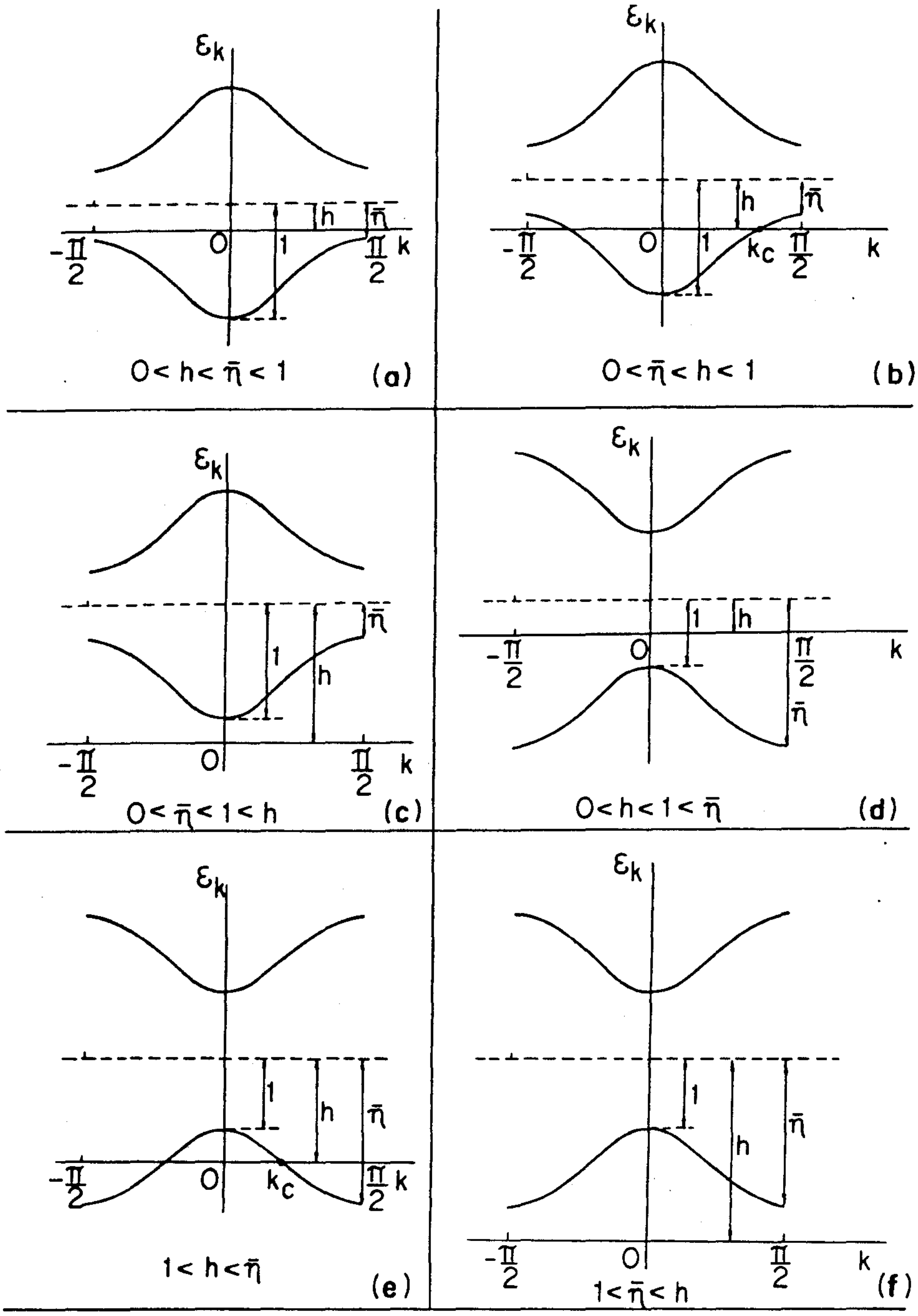

FIG.8

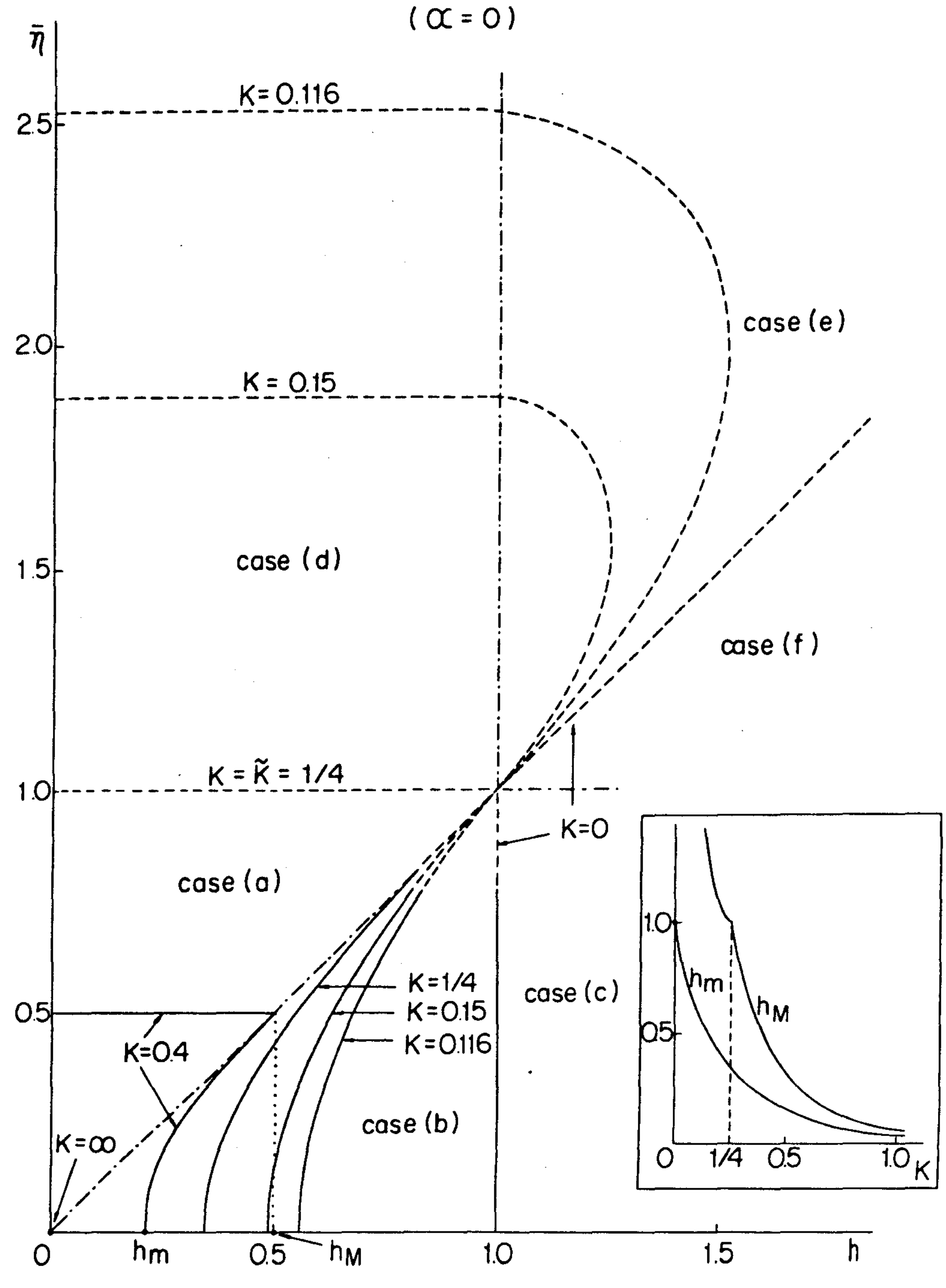

(α = 0)
$\bar{\eta}$
K= 0.116
2.5
case (e)
2.0
K = 0.15
case (d)
1.5
case (f)
K = $\tilde{K}$ = 1/4
1.0
K=0
case (a)
K=1/4
K=0.15
K=0.116
case (c)
0.5
K=0.4
K=∞
case (b)
0
hm
0.5
hM
1.0
1.5
h
1.0
0.5
hm
hM
0
1/4
0.5
1.0
K

FIG. 9

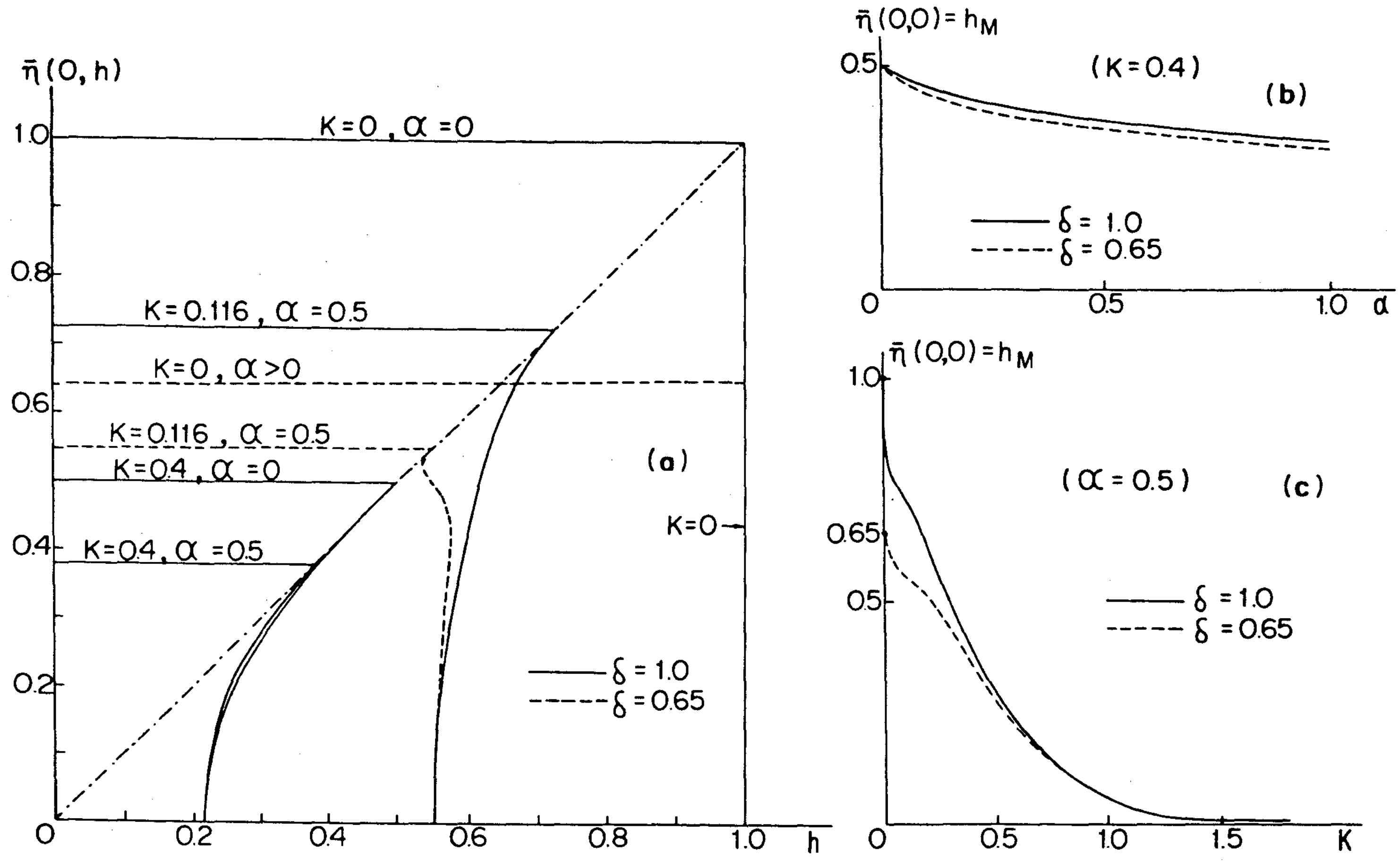

η̄ (0, h)
1.0
0.8
0.6
0.4
0.2
0
K=0 , α =0
K=0.116 , α =0.5
K=0 , α >0
K=0.116 , α =0.5
K=0.4 , α =0
K=0.4 , α =0.5
(a)
K=0
δ = 1.0
δ = 0.65
0.2
0.4
0.6
0.8
1.0
h
η̄ (0,0) = h_M
0.5
(K=0.4)
(b)
δ = 1.0
δ = 0.65
0
0.5
1.0
α
η̄ (0,0) = h_M
1.0
0.65
0.5
(α = 0.5)
(c)
δ = 1.0
δ = 0.65
0
0.5
1.0
1.5
K

FIG.10

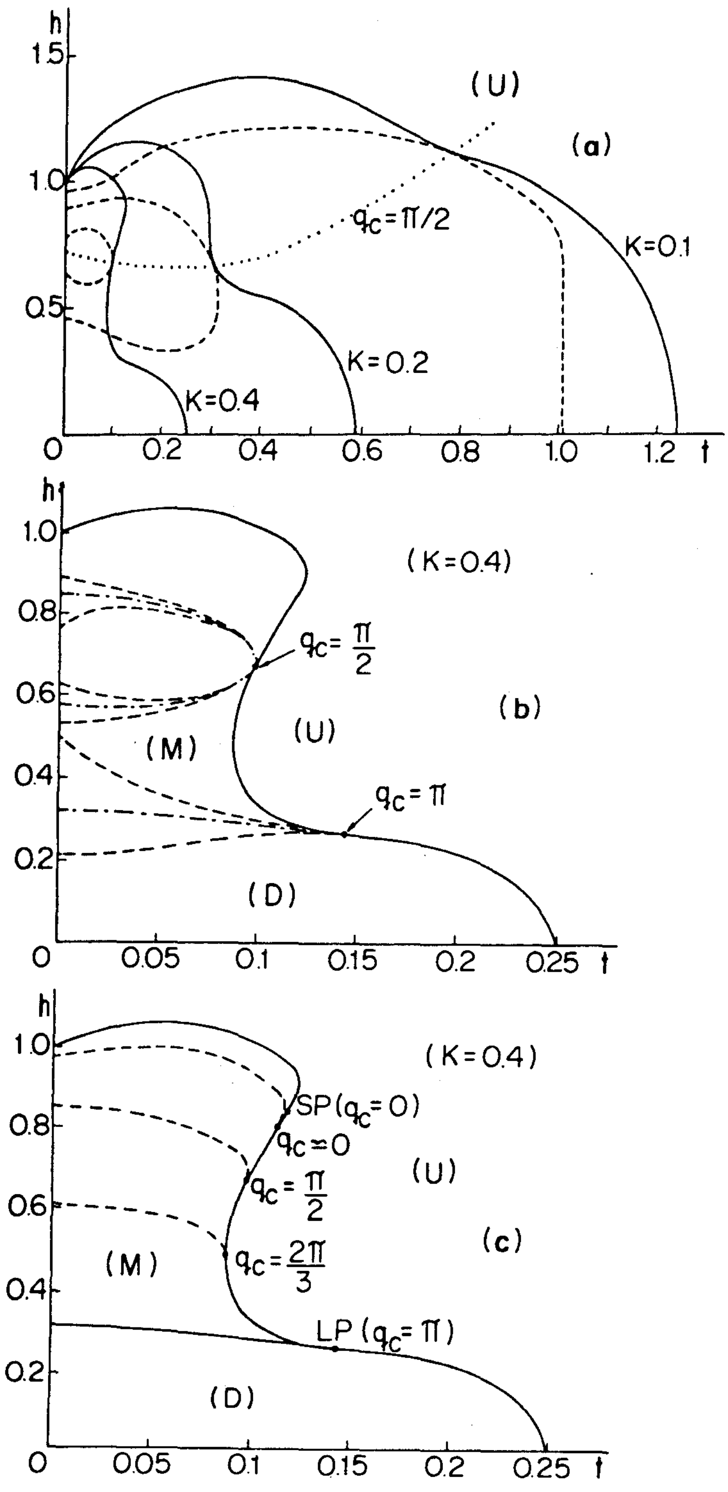

(U)
(a)
$q_c = \pi/2$
K=0.1
K=0.2
K=0.4
(K=0.4)
$q_c = \frac{\pi}{2}$
(b)
(M)
(U)
$q_c = \pi$
(D)
(K=0.4)
SP (q_c=0)
$q_c \simeq 0$
(U)
$q_c = \frac{\pi}{2}$
(c)
(M)
$q_c = \frac{2\pi}{3}$
LP ($q_c = \pi$)
(D)

FIG.11

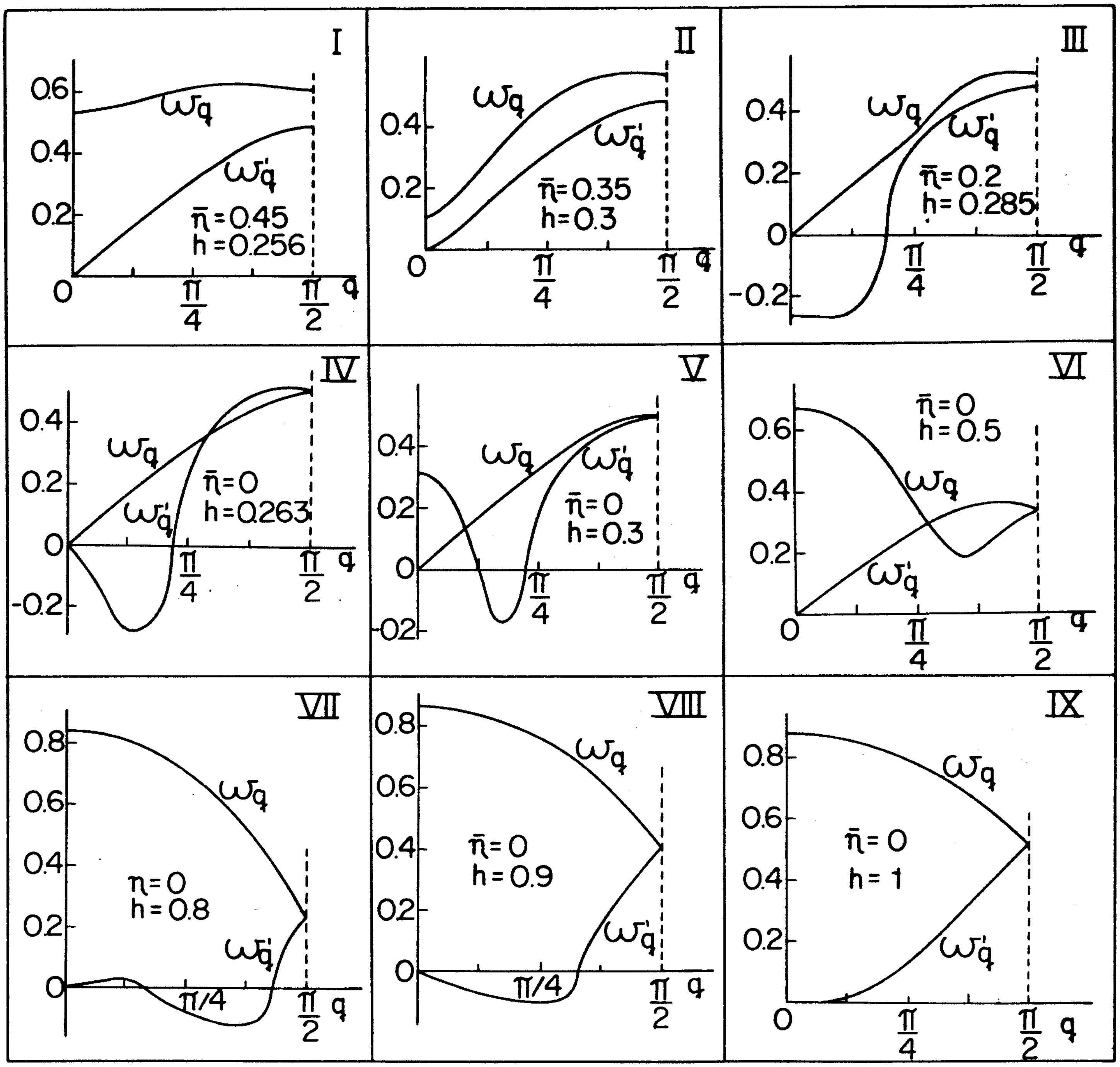
I
ω_q
ω'_q
$\bar{n}=0.45$
$h=0.256$
II
$\bar{n}=0.35$
$h=0.3$
III
$\bar{n}=0.2$
$h=0.285$
IV
$\bar{n}=0$
$h=0.263$
V
$\bar{n}=0$
$h=0.3$
VI
$\bar{n}=0$
$h=0.5$
VII
$n=0$
$h=0.8$
VIII
$\bar{n}=0$
$h=0.9$
IX
$\bar{n}=0$
$h=1$
$\pi/4$
$\pi/2$
q

FIG. 12

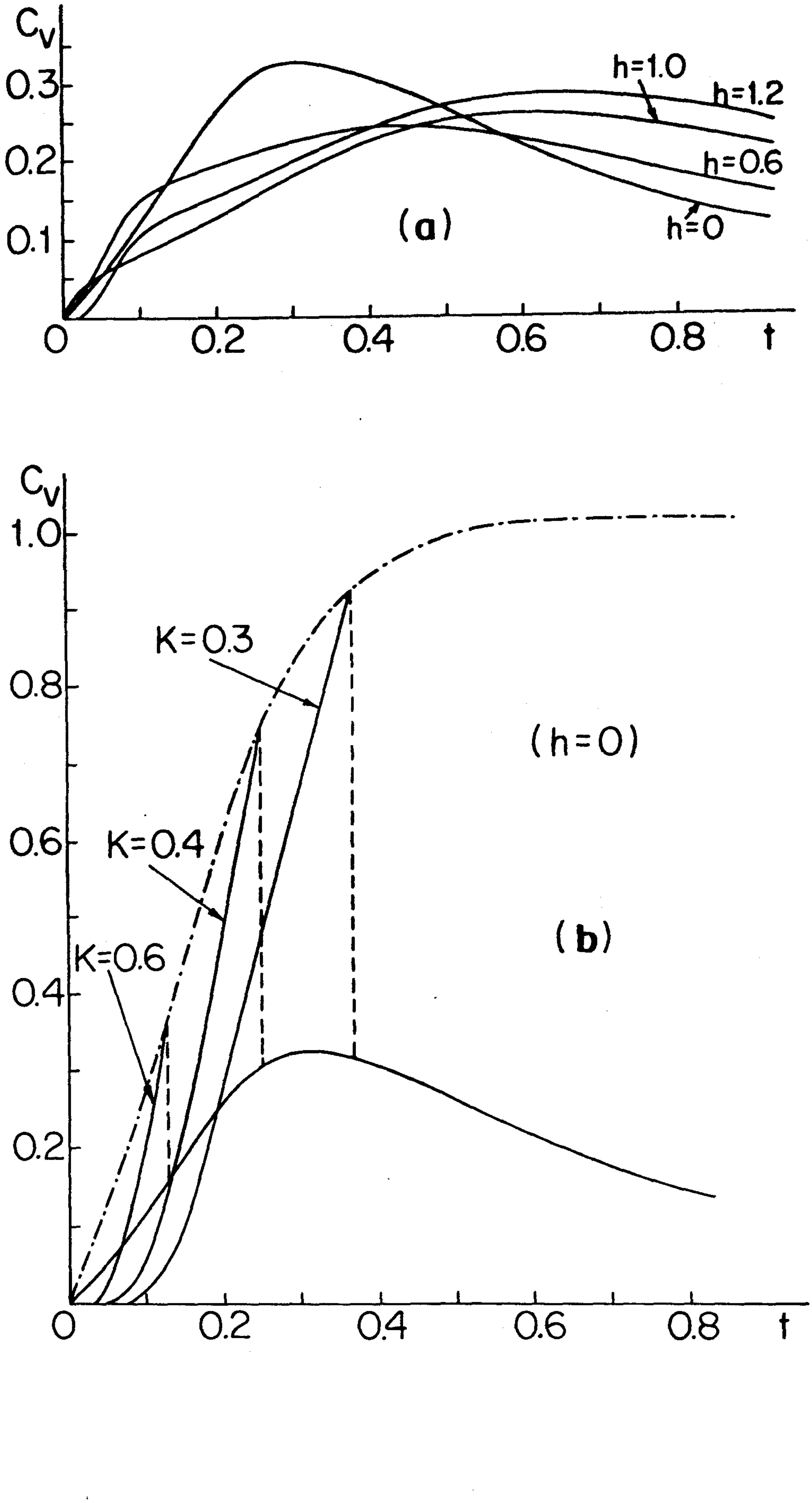

Cv
0.3
0.2
0.1
0
0.2
0.4
0.6
0.8
t
h=1.0
h=1.2
h=0.6
h=0
(a)
Cv
1.0
0.8
0.6
0.4
0.2
0
0.2
0.4
0.6
0.8
t
K=0.3
K=0.4
K=0.6
(h=0)
(b)

FIG.13

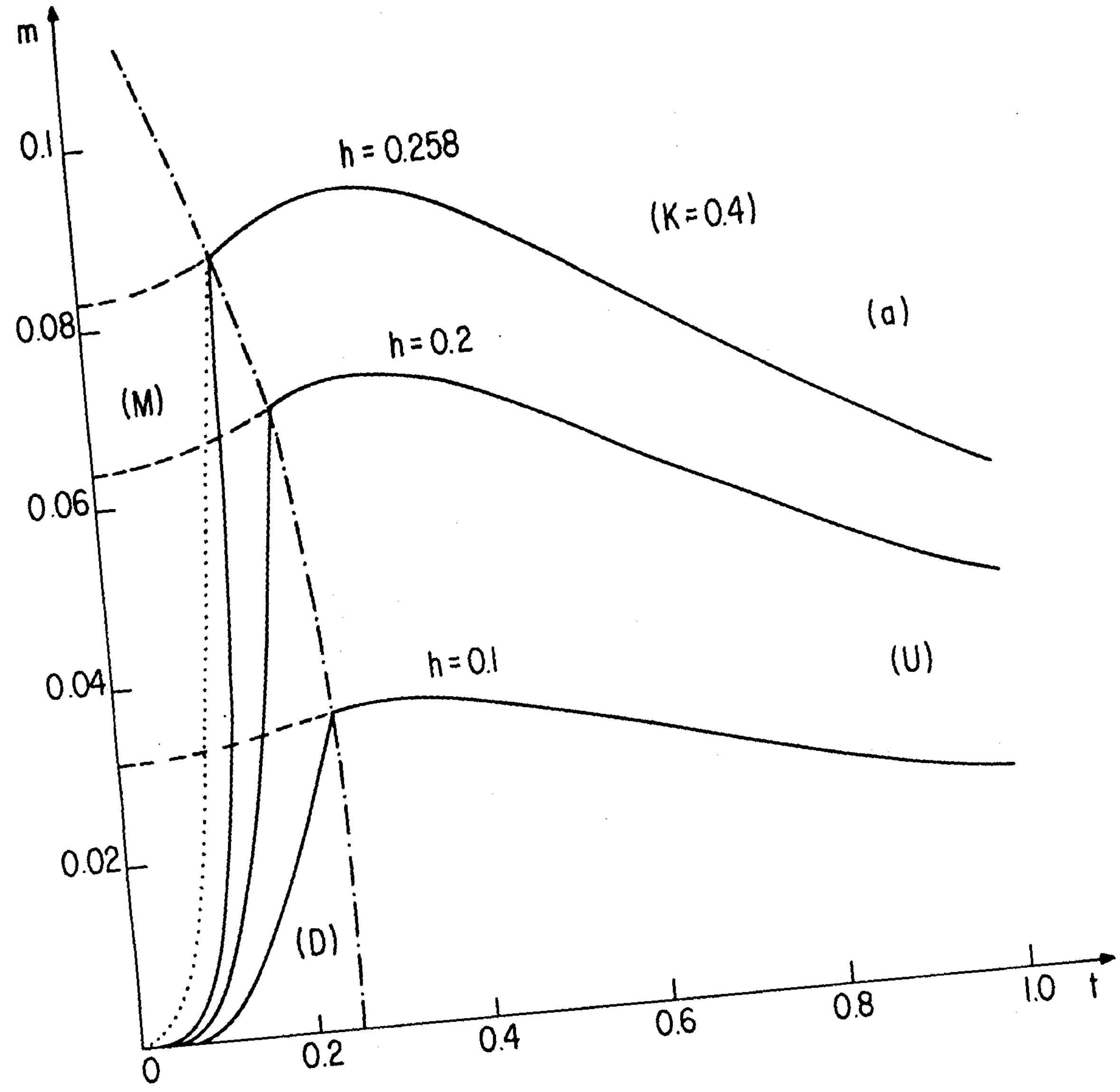

FIG.14

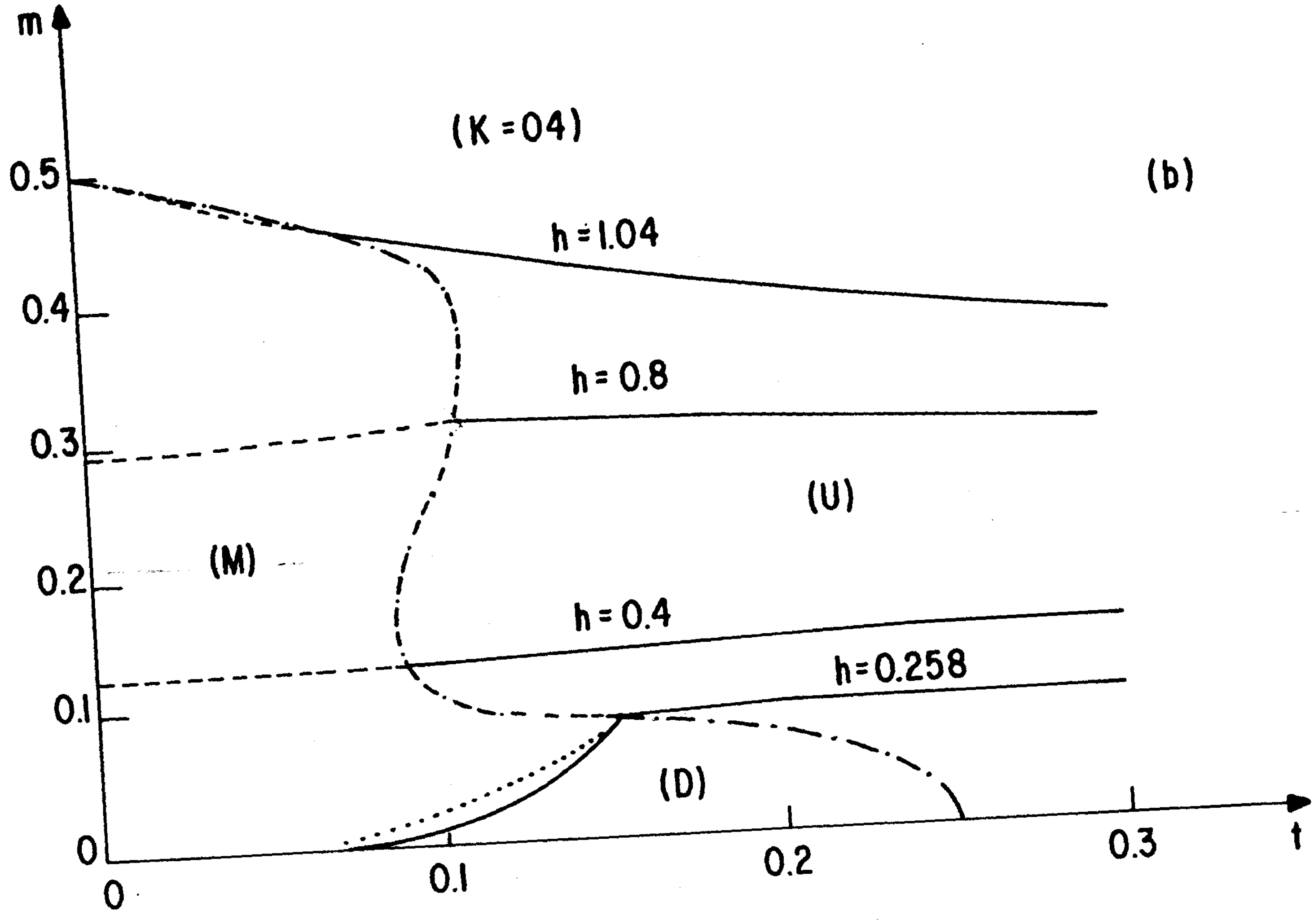

FIG. 14

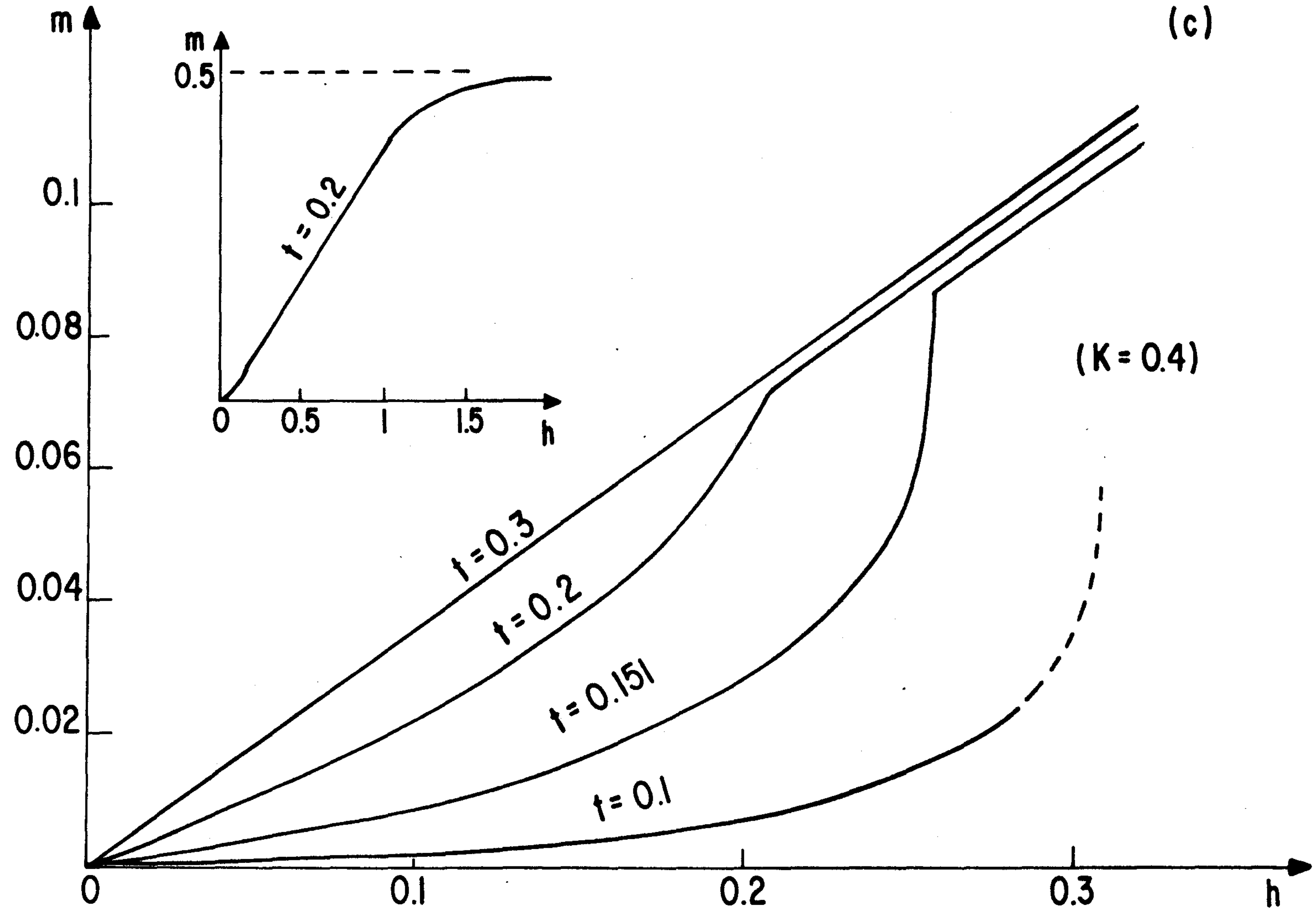
(c)
m
0.1
0.08
0.06
0.04
0.02
0
0.1
0.2
0.3
h
(K = 0.4)
t = 0.3
t = 0.2
t = 0.151
t = 0.1
m
0.5
t = 0.2
0
0.5
1
1.5
h

FIG. 14

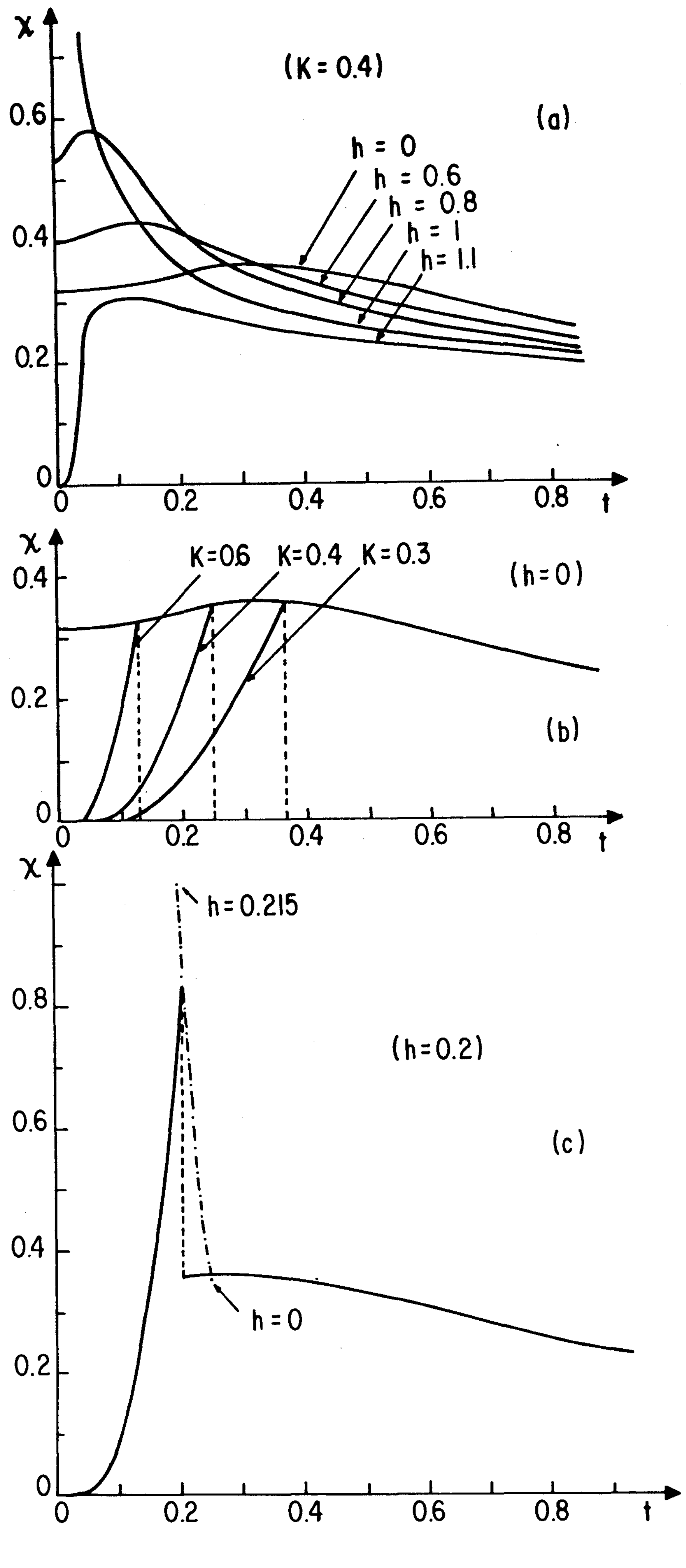

χ
(K = 0.4)
(a)
0.6
0.4
0.2
0
h = 0
h = 0.6
h = 0.8
h = 1
h = 1.1
0
0.2
0.4
0.6
0.8
t
χ
K=0.6
K=0.4
K=0.3
(h=0)
(b)
χ
h=0.215
(h=0.2)
(c)
h=0

FIG.15

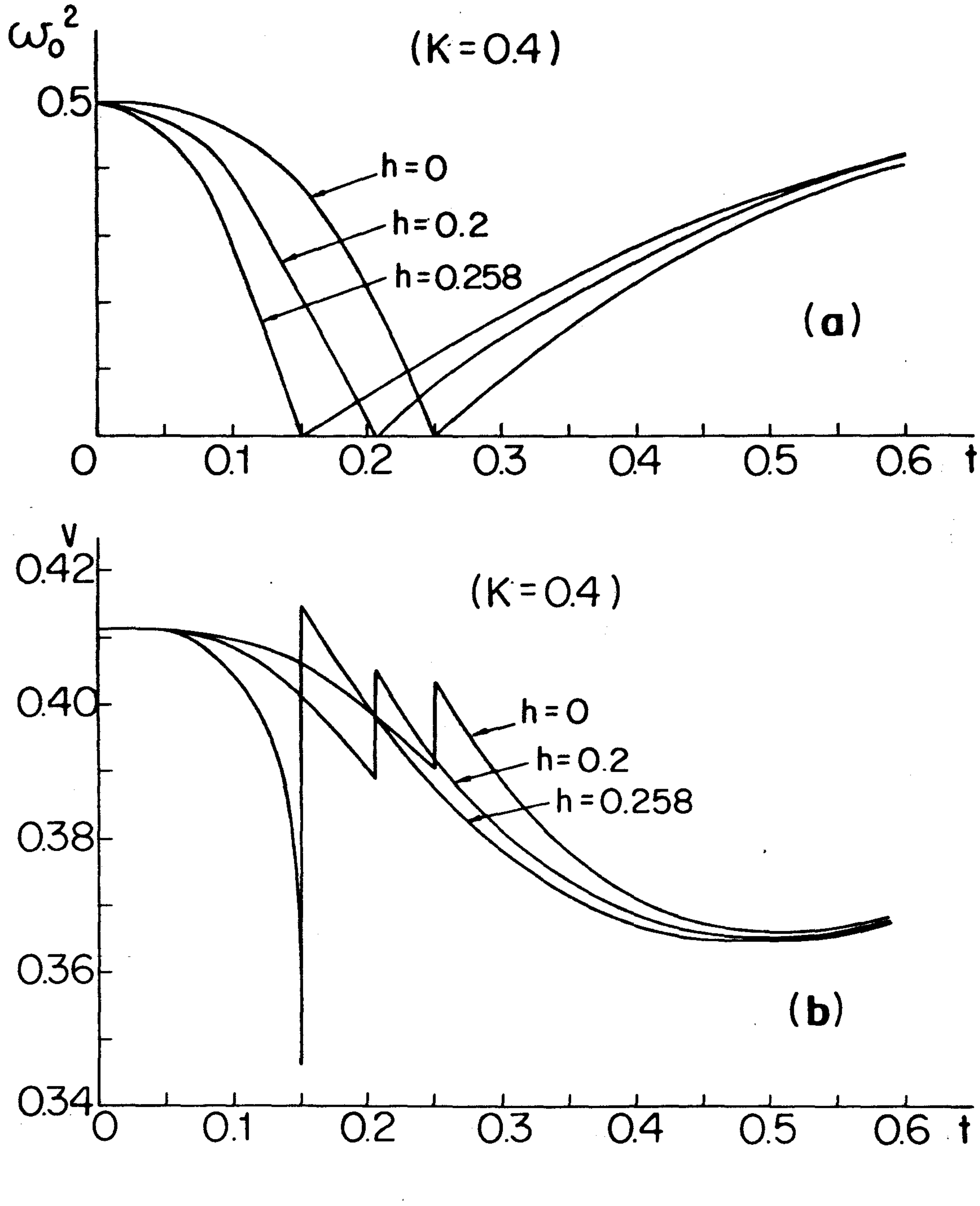

ω_0^2
(K=0.4)
0.5
h=0
h=0.2
h=0.258
(a)
0
0.1
0.2
0.3
0.4
0.5
0.6
t
V
0.42
(K=0.4)
0.40
h=0
h=0.2
h=0.258
0.38
0.36
(b)
0.34
0
0.1
0.2
0.3
0.4
0.5
0.6
t

FIG. 16